


1-1-2007

Dynamic Stereochemical Rearrangements in Chiral Organometallic

Peter J. Heard

Glyndwr University, p.heard@glyndwr.ac.uk

Follow this and additional works at: <http://epubs.glyndwr.ac.uk/chem>

 Part of the [Inorganic Chemistry Commons](#), [Organic Chemistry Commons](#), and the [Physical Chemistry Commons](#)

Copyright © 2007 RCS, and reproduced here by permission of The Royal Society of Chemistry (RSC). This is the author's final draft after peer review. The article was published in Heard, P. J. (2007) 'Dynamic Stereochemical Rearrangements in Chiral Organometallic Complexes'. *Chemical Society Reviews*, 36(3), 551-569 by the Royal Society of Chemistry and the published version is available online at <http://www.rsc.org>

Recommended Citation

Heard, P. J. (2007) 'Dynamic Stereochemical Rearrangements in Chiral Organometallic Complexes'. *Chemical Society Reviews*, 36(3), 551-569

This Article is brought to you for free and open access by the Materials Science at Glyndŵr University Research Online. It has been accepted for inclusion in Chemistry by an authorized administrator of Glyndŵr University Research Online. For more information, please contact d.jepson@glyndwr.ac.uk.

Dynamic stereochemical rearrangements in chiral organometallic complexes†

Peter J. Heard

Received 26th April 2006

First published as an Advance Article on the web 17th July 2006

DOI: 10.1039/b514855n

Organometallic complexes have long been known to display a wide variety of dynamic stereochemical processes. Classic examples of such processes include the exchange of axial and equatorial environments in trigonal bipyramidal complexes, such as $\text{Fe}(\text{CO})_5$, and the migration of the metal moiety round the periphery of the cyclopentadiene ring in η^1 -bound Cp complexes. The systematic study of fluxional processes is of interest because it can not only help provide a detailed, quantitative 'picture' of the bonding between the metals and ligands involved, but it can also help to rationalise chemical reactivity patterns. The introduction of chirality into organometallic complexes, usually in the form of a non-racemic chiral ligand, has led to an explosion in the importance such species, particularly with regard to their applications in organic functional group transformations. The presence of a chiral centre can also provide an excellent spectroscopic handle on the complex in question, enabling both novel fluxional processes to be observed and new light to be shed on old (unresolved) problems. In this *critical review* (101 references) the literature on metal-centred fluxional rearrangements in chiral transition and main group organometallic complexes is reviewed, complementing the recent review by Faller (see reference 8).

Introduction

Molecules that alternate between discrete structures are said to be stereochemically non-rigid or fluxional. Strictly, the term *fluxional* applies only to stereochemical rearrangements between structures that are chemically indistinguishable (*i.e.* degenerate). This distinction is now generally ignored and dynamic processes are widely referred to as fluxional

processes, irrespective of whether or not the species involved are degenerate.

The examples of PF_5 and $\text{Fe}(\text{CO})_5$ are often given at undergraduate level to introduce the idea of dynamic stereochemical behaviour. If the structures were static on the NMR chemical shift time-scale two separate resonances would be expected in an intensity ratio of 2 : 3, for the axial and equatorial positions, respectively. That only one signal is observed clearly indicates the existence of some dynamic process that rapidly interconverts axial and equatorial positions. The classic mechanism used to rationalise this observation is the Berry twist¹ (Scheme 1), although this is not the only mechanism that can be envisaged for this type of rearrangement.

Since the emergence of NMR spectroscopy as a routine technique, it has become apparent that fluxionality is a common feature of many inorganic and organic compounds, and a wide variety of fluxional processes have been identified in such species, particular in transition metal organometallic complexes.^{2–8} Classic examples include the inversion of configuration at metal co-ordinated sulfur atoms

School of Biological and Chemical Sciences, Birkbeck University of London, Malet Street, London, UK WC1E 7HX.

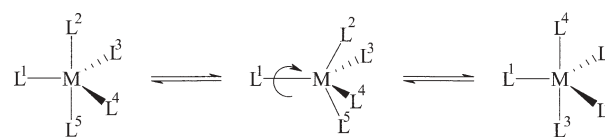
E-mail: p.heard@bbk.ac.uk; Fax: 0207 631 6246; Tel: 0207 079 0795

† Dedicated to the memory of Dr Vladimir Šik, who made an outstanding contribution to the development of dynamic NMR methods and the study of fluxional organometallic complexes.

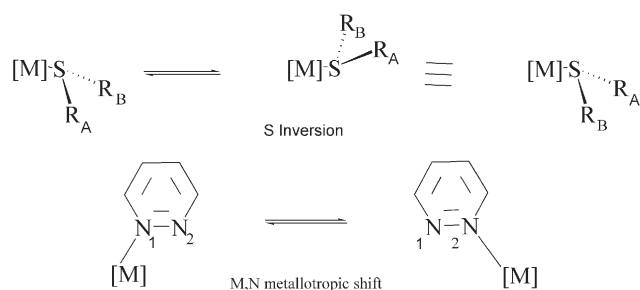


Peter Heard

Peter Heard received his BSc from the University of Durham in 1991 then move to the University of Exeter where he completed his PhD under the supervision of Professor Edward W. Abel in 1994. After spending a year as a post-doctoral fellow working with Professor J. W. Faller at Yale University, he returned to the UK to take up a temporary lectureship in inorganic chemistry at the University of Wales Swansea. He moved to his present position at Birkbeck University of London in 1996.



Scheme 1 Berry pseudo-rotation in trigonal bipyramidal ML_5 complexes.



Scheme 2 Sulfur inversion and metallotropic shift processes in transition metal complexes.



Scheme 3 1,3-M,C metallotropic shift in allyl Grignard reagents.

and metallotropic shifts between different donor groups of a ligand (Scheme 2). The study of dynamic processes can provide detailed quantitative information on the interactions between the ligands and the metal centre and can also aid our understanding of chemical behaviour. For example the reaction of substituted allyl Grignard reagents with alkyl halides often gives a mixture of products. The occurrence of different products can be understood when it is realised that the Grignard reagent is fluxional, as shown in Scheme 3. Reaction of the two discrete structural forms in Scheme 3 with the alkyl halide gives two different products.

As many fluxional processes involve quite significant changes in geometry or even the breaking and reforming of bonds, the activation barriers are often fairly high. For organometallic complexes the free energies of activation lie typically in the range 20–120 kJ mol⁻¹. Given the relatively high energy barriers (hence slow rates) and the presence of organic ligands, such processes are ideally suited to investigation by nuclear magnetic resonance methods. A number of ‘dynamic NMR’ (DNMR) experiments have been developed that can provide both a qualitative *picture* of the stereodynamics and a quantitative evaluation of the exchange rates. The most widely applicable techniques are summarised in Table 1.

Although the various DNMR methodologies have been reviewed extensively elsewhere,^{2,4,5,9} there are a number of important aspects, particularly regarding selection of technique, that merit reiterating here.

In general, band shape analysis is the preferred technique because it permits the widest range of rates to be determined,

allowing a more accurate estimate of the activation parameters *via* the Eyring equation, (1).

$$\ln(k/T) = (-\Delta H/RT) + (\Delta S/R) + \ln(k_b/h) \quad (1)$$

The acquisition of good quality rate data can be expensive in both spectrometer time and spectral analysis (see below), so many workers opt to obtain an estimate of the free energy of activation (ΔG^\ddagger) at a single temperature. Estimates are most usually made from coalescence temperature (T_c) measurements using eqn (2):

$$\Delta G(T_c) = -RT_c \ln(\pi \Delta\nu h / k_b T_c \sqrt{2}) \quad (2)$$

$\Delta\nu$ is the separation (in Hz) between exchanging resonances.

Alternatively, ΔG^\ddagger can be estimated from the temperature, T_i , at which observable line broadening first occurs using eqn (3):

$$G(T_i) = -RT_i \ln(\pi W h / k_b T_i) \quad (3)$$

ΔW is the exchange induced excess line width.

From eqn (2), it can be seen that the temperature at which coalescence occurs depends on the separation of the exchanging signal (expressed in Hz) and hence, where chemical shifts are exchanged, on the basic operating frequency of the spectrometer. Comparison of barriers calculated using this method can thus be quite misleading and this author supports the recommendation of Faller^{6,8} that estimates based on initial band broadening are preferable.

The acquisition of high quality DNMR spectra suitable for band shape analysis (BSA) requires precise control of probe temperature (to ± 1 °C) and sufficient time must be allowed for the sample to equilibrate (this author recommends not less than 10 min). Spectra should be recorded at 5–10 degree intervals over as wide a temperature range as possible. Field inhomogeneities should be minimised at each temperature. This is best done with reference to an internal standard that possesses relatively temperature-independent parameters and is not in anyway involved in the dynamic process. Finally it is important to get a good assessment of how the static NMR parameters vary with temperature, as this information is required in the line shape analysis, for which many programs are currently available.⁸

Rate processes that are slow on the chemical shift/scalar couplings time-scales may still be quite fast on the spin–dash relaxation time-scale. Such processes can be observed using

Table 1 NMR time-scales and common dynamic NMR methods

NMR parameter modulated	Approximate time-scale/s	DNMR technique	Measurable rates/s ⁻¹
Chemical shifts	$\sim 4 \times 10^{-4}$	Band shape analysis ^a (BSA)	5×10^0 – 5×10^3
Scalar couplings	$\sim 4 \times 10^{-4}$	Band shape analysis ^a (BSA)	5×10^0 – 5×10^3
T_1 Relaxation times	2×10^{-1} – 1×10^{-1}	1D saturation transfer ^b (SAT)	5×10^{-2} – 1×10^1
	2×10^{-1} – 1×10^{-1}	2D exchange spectroscopy ^b (EXSY)	5×10^{-2} – 1×10^1
Signal intensities	1×10^2 – 1×10^4	Time-dependent studies ^c	1×10^{-4} – 1×10^{-2}

^a The actual range accessible by BSA depends on the separation of the exchanging signals, expressed in Hz. The range of rates accessible on the chemical shift time-scale therefore depends on both the observed nuclide and the operating frequency of the spectrometer. The range of rates accessible on the scalar couplings time-scale depends on $|J_{ij}|$. ^b Exchange must be slow on the chemical shift and scalar coupling constant time-scales. ^c Non-equilibrium studies.

magnetisation transfer methods, based on both 1D and 2D nuclear Overhauser experiments. One-dimensional selective inversion experiments are generally preferable as the integration of the signal intensities is more reliable. Although Bain⁹ has developed methods that can be applied to spin coupled systems, the use of quantitative 1D exchange experiments remains largely confined to uncoupled systems. Another drawback of the 1D technique is that only exchanges involving the perturbed resonance can be observed (although this can be put to good advantage). Thus for multi-site exchanges and/or those involving coupled signals, the 2D variant (2D EXSY) is generally employed. Both the 1D and 2D experiments may be complicated by cross-relaxation effects. Any potential problems can be overcome largely by the judicious choice of observed nuclide: dilute nuclides are preferred. In EXSY, NOE peaks can usually be distinguished from exchange peaks using phase-sensitive experiments: exchange peaks are positive while, for small organometallic complexes in mobile solvents, NOE peaks are negative.

The study of chemical exchange phenomena by NMR requires that one or more of the basic parameters that characterise the spectrum is modulated by the exchange processes. Any process that does not affect at least one of the parameters will be invisible to the NMR experiment.

The introduction of a chiral centre reduces the molecular symmetry, opening up the possibility of observing fluxional processes that would otherwise be NMR 'invisible'. The use of chiral complexes for the elucidation of novel fluxional processes is illustrated by the example of $[\text{Zr}\{\text{C}_2\text{H}_4(\text{THInd})_2\}\text{Me}(\text{BPh}_4)]$ (THInd = tetrahydroindenyl).¹⁰ The low temperature limiting ¹H NMR spectrum displays five equally intense signals from the hydrogens of the metal-bound phenyl ring of the tetrafluoroborate ligand. On warming, the spectrum collapses to an AB₂C₂ pattern as a result of a dynamic process that rapidly exchanges the two *ortho* and two *meta* resonances. The fluxional process (Scheme 4) is only observable because of the asymmetry at zirconium.

The presence of a chiral centre can also enable different possible mechanistic pathways to be distinguished. The metallotropic shift of the cyclopentadiene ligand in $\eta^1\text{-Cp}$ complexes, which results in a single signal being observed for the ring hydrogen atoms in the fast exchange regime was identified early in the study of fluxional organometallic compounds. A 1,2-M,C shift was postulated, but it is difficult to distinguish from a 1,3-M,C shift because the 2 and 5, and 3 and 4 cyclopentadiene ring positions are equivalent. If a chiral metal centre is employed this equivalence is broken and five signals are observed in slow exchange limit. The two possible pathways are thus distinguished more easily by line shape analysis, confirming a concerted 1,2-M,C shift was

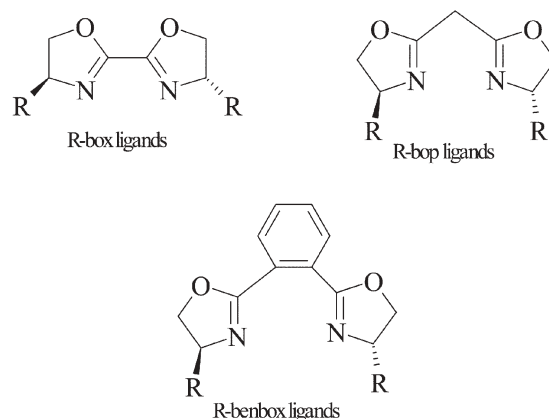


Fig. 1 C₂-Symmetric bis(oxazoline) ligands.

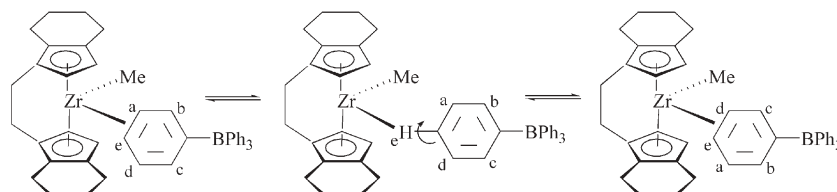
involved.¹¹ This study exemplifies clearly how the presence of a chiral centre can be used to differentiate readily between possible fluxional pathways.

Fluxional complexes of labile ligands

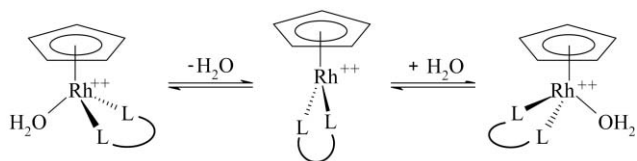
A key step in the 'initiation' of a fluxional process in an organometallic complex may be the (reversible) loss of a weakly bound ligand, thereby creating a coordinatively unsaturated metal centre with a more dynamic geometry.

The loss of the C₂-symmetry of the bis(oxazoline) ligands shown in Fig. 1, which occurs on complexation to the $[\text{RhCp}^*\text{Cl}]^+$ (Cp* = $\eta^5\text{-C}_5\text{Me}_5$) moiety is clearly revealed by the inequivalence of all of the ligand-hydrogens in the ambient temperature ¹H NMR spectra of the complexes. The corresponding spectra of the dicationic aquo-adducts $[\text{RhCp}^*(\text{H}_2\text{O})(\text{N},\text{N})]^{2+}$ (N,N = ⁱPr-box or ⁱPr-bop) are more simple, and show that the ligand possesses (average) C₂-symmetry.¹² This apparent C₂-symmetry can be rationalised by a dynamic process that effectively 'flips' the co-ordinated oxazoline ligand over. The ¹H NMR spectra of the aquo complexes also indicate reversible co-ordination of the water molecule. Although the rates of exchange of water and the 'flip' of the oxazoline are similar in the box and bop complexes, the exchange of the oxazoline signals in the benbox complex, $[\text{RhCp}^*(\text{H}_2\text{O})(\text{benbox})]^{2+}$, is clearly much the slower process.

Identical behaviour is observed in the $[\text{Ru}(\text{arene})(\text{H}_2\text{O})(\text{bop})]^{2+}$ complexes,^{13,14} but the free energies of activation are higher. The metal dependence of the rates is in accord with the relative rates of water exchange (*i.e.* Rh > Ru), and indicate that dissociation of water is necessary for the dynamic process



Scheme 4 Proposed mechanism of phenyl ring rotation in $[\text{Zr}\{\text{C}_2\text{H}_4(\text{THInd})_2\}\text{Me}(\text{BPh}_4)]$ (THInd = tetrahydroindenyl).



Scheme 5 Probable ligand flip mechanism in $[\text{RhCp}(\text{H}_2\text{O})\text{bis}(\text{oxazoline})]^{2+}$ and analogous complexes. This mechanism also leads to inversion of configuration at the metal atom.

to proceed. A number of possible mechanisms have been identified and investigated in detail by Corminboeuf, Frey and Kündig,¹⁵ who concluded that a dissociative pathway *via* a pseudo trigonal planar transition state, depicted in Scheme 5, is most likely. This mechanism, which also results in inversion of configuration at the metal, is in accord with theoretical studies on model 16-electron two-legged piano stool complexes that show the barrier to inversion at the metal centre is quite low in such species ($<63 \text{ kJ mol}^{-1}$).¹⁶

In complexes of C_2 -symmetric ligands, such as bis(oxazoline) ligands, inversion of configuration at the metal does not lead to any change in the stereochemical environment at the metal. This retention of the stereochemical environment is important because Lewis acidic Rh and Ru $[\text{M}(\eta^5\text{-C}_n\text{H}_n)(\text{N},\text{N})\text{L}]^+$ (L = labile ligand) complexes can catalyse asymmetric Diels–Alder additions.^{12–15,17,18} If a non- C_2 -symmetric ligand is employed the fluxionality leads to a change in the stereochemical environment at the metal, degrading enantioselectivity.¹⁹

Brunner has shown that, contrary to earlier reports, the metal centre is similarly configurationally labile in $[\text{M}(\eta^5\text{-C}_n\text{R}_n)\text{L}]$

($\text{M} = \text{Ru}, \text{Rh}$ or Ir ; $n = 5, \text{R} = \text{H}$ or Me ; $n = 6, \text{R} = \text{H}$; L = monodentate ligand) complexes of optically active bidentate Schiff base pyrrolecarbaldiminato and salicylaldiminato ligands.^{20–23} Free energies of activation are reported in Table 2, along with those for the bis(oxazoline) complexes (above) and for the epimerisation of the metal centre in the ‘purely’ tetrahedral $[\text{Co}(\text{CO})(\text{NO})(\text{L},\text{L}^*)]$ and $[\text{Co}(\text{CO})(\text{NO})(\text{L})(\text{L}^*)]$ complexes (L,L^* = chiral bidentate ligand; L^* = chiral monodentate ligand).^{24,25}

Although there is considerable variation in the free energies of activation, depending on the nature of both the labile ligand and ancillary ligands, examination of Table 2 reveals that, with respect to the metal, the general trend is $\text{Co} > \text{Ru} > \text{Rh} \approx \text{Ir}$, presumably indicating the relative lability of ligands on these metal centres.

Fluxional complexes of hemilabile ligands

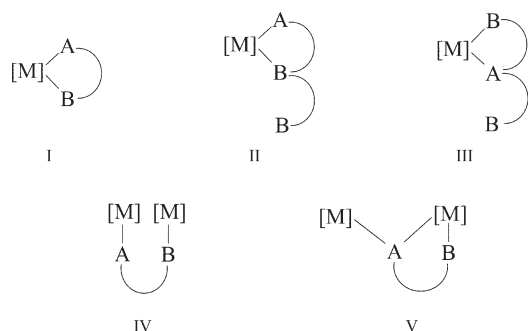
Hemilabile ligands are polydentate ligands that contain at least two different functionalities, one of which is substantially labile. Braunstein also suggested²⁶ that the labile functionality must exhibit fully reversible bond rupture/re-coordination. For this to be the case the energy difference between the coordinated and unbound (or ‘closed’ and ‘open’) forms must be relatively small. In many cases the energy difference between the two forms is sufficiently small for both species to be observed in the NMR experiment. Thus, provided the activation energy for the ‘opening’ is within the range amenable to NMR, the structural dynamics of the hemilabile ligand can be observed.

The structural dynamics of hemilabile ligands can have significant effects on the chemical reactivity of the complexes:

Table 2 Gibbs free energies of activation^a for the inversion of configuration at the metal centre in tetrahedral and pseudo tetrahedral complexes with labile ligands

Complex ^b	$\Delta G^\ddagger/\text{kJ mol}^{-1}$	Reference
$[\text{Co}(\text{CO})(\text{NO})\{\text{P}(\text{OMe})_3\}\{\text{PPH}_2\text{N}(\text{Me})-(S)\text{-CH}(\text{Ph})\text{Me}\}]$	126.3	24
$[\text{Co}(\text{CO})(\text{NO})(\text{PPh}_3)\{\text{CN}-(S)\text{-CH}(\text{Ph})\text{Me}\}]$	112.4	24
$[\text{Co}(\text{CO})(\text{NO})(\text{PMe}_2\text{Ph})\{(R)\text{-glyphos}\}]$	111.7	24
$[\text{Co}(\text{CO})(\text{NO})(\text{LL}-2)]$	88.1 (406 K)	25
$[\text{Co}(\text{CO})(\text{NO})(\text{LL}-1)]$	87.5 (406 K)	25
$[\text{Co}(\text{CO})(\text{NO})\{(R)\text{-prophos}\}]$	<i>ca.</i> 84	25
$[\text{Co}(\text{CO})(\text{NO})\{(S,S)\text{-norphos}\}]$	<i>ca.</i> 84	25
$[\text{RuCp}\{(S)\text{-LL}-3\}(\text{PPh}_3)]$	<i>ca.</i> 110	23
$[\text{Ru}(\text{benzene})(\text{OH})\{(S)\text{-Ph-bop}\}]^{2+}$	$>80^c$	13
$[\text{Ru}(\text{benzene})(4\text{-Mepy})\{(S)\text{-LL}-4\}]^{2+}$	<i>ca.</i> 75 (238 K) ^c	21
$[\text{Ru}\{(S)\text{-}^i\text{Pr-bop}\}(\text{mes})(\text{OH}_2)]^{2+}$	>70 (<i>ca.</i> 298 K) ^c	14
$[\text{Ru}(\text{acetone})\{(S)\text{-}^i\text{Pr-bop}\}(\text{mes})]^{2+}$	≤ 69 (<i>ca.</i> 298 K) ^c	14
$[\text{Ru}(\text{benzene})\{(S)\text{-Ph-bop}\}(\text{OH}_2)]^{2+}$	64.5 ($\text{d}_6\text{-acetone}$)	13
	55.6 (CD_2Cl_2)	13
$[\text{Ru}(\text{benzene})(\text{OH})\{(S)\text{-Ph-bop}\}]^{2+}$	>80 (328 K) ^c	13
$[\text{RuCp}\{(R)\text{-BINOP-F}\}(\text{H}_2\text{O})]^{2+}$	50.7	15
$[\text{Ru}\{(S)\text{-}^i\text{Pr-bop}\}(\text{mes})(\text{OH}_2)]^{2+}$	<i>ca.</i> 50 (233 K) ^c	14
$[\text{RhCp}^*\{(S)\text{-}^i\text{Pr-benbox}\}(\text{H}_2\text{O})]^+$	>70 (273 K) ^c	12
$[\text{RhCp}^*\text{Cl}\{(S)\text{-LL}-4\}]$	<i>ca.</i> 60 (294 K) ^c	20
$[\text{RhCp}^*\{(S)\text{-}^i\text{Pr-bop}\}(\text{H}_2\text{O})]^+$	<i>ca.</i> 50 (223 K) ^c	12
$[\text{RhCp}^*\{(S)\text{-}^i\text{Pr-bop}\}(\text{H}_2\text{O})]^+$	≤ 50 (213 K) ^c	12
$[\text{RhCp}^*\text{Cl}\{(S)\text{-LL}-3\}]$	<i>ca.</i> 25 (223 K) ^c	20
$[\text{IrCp}^*\text{Cl}\{(S)\text{-LL}-4\}]$	<i>ca.</i> 56 (271 K) ^c	20
$[\text{IrCp}^*\text{Cl}\{(S)\text{-LL}-3\}]$	<i>ca.</i> 26 (233 K) ^c	20

^a ΔG^\ddagger reported at 298 K unless otherwise stated. ^b Ligand abbreviations: glyphos = (4,4-dimethyl-1,3-dioxolan-2-yl)methyldiphenylphosphane; prophos = 1,2-bis(diphenylphosphanyl)propane; norphos = 5,6-bis(diphenylphosphanyl)bicyclo[2.2.1]hept-2-ene; LL-1 = *N*-methyl(2-pyridinylmethylene)benzenemethanamine; LL-2 = *N*-methyl-[1-(2-pyridinyl)ethylidene]benzenemethanamine; LL-3 = anion of 2-*N*-[1-phenylethyl]pyrrolecarbaldimine; LL-4 = anion of *N*-(1-phenylethyl)salicylideneamine. ^c Estimated from the low temperature limiting ¹H NMR spectra or *t*_{1/2} data reported in the primary source.



Scheme 6 Examples of hemilabile ligand bonding modes (see reference 26 for a more extensive list).

these effects may be adventitious (*e.g.* freeing up a co-ordination site on the metal) or detrimental (*e.g.* reducing the regio- and/or stereo-selectivity). The effects of hemilability on chemical reactivity have been discussed in the review by Braunstein and Naud.²⁶ Here, the focus is on the details of the structural dynamics.

Hemilabile ligands can adopt a variety of bonding modes, depending on the denticity of the ligand itself and the nature of the metal moiety to which it is co-ordinated. Those bonding modes pertinent to this review are depicted in Scheme 6.²⁶ In type II and III complexes the ligands possess a pendant (or redundant) donor atom which is not bound to the metal. In such complexes the pendant donor group can (potentially) exchange with one of the co-ordinated groups. In type I, III and IV complexes all of the donor groups are co-ordinated, but reversible on/off co-ordination of one of the donors can occur, sometimes with the initiation of further stereochemical changes.

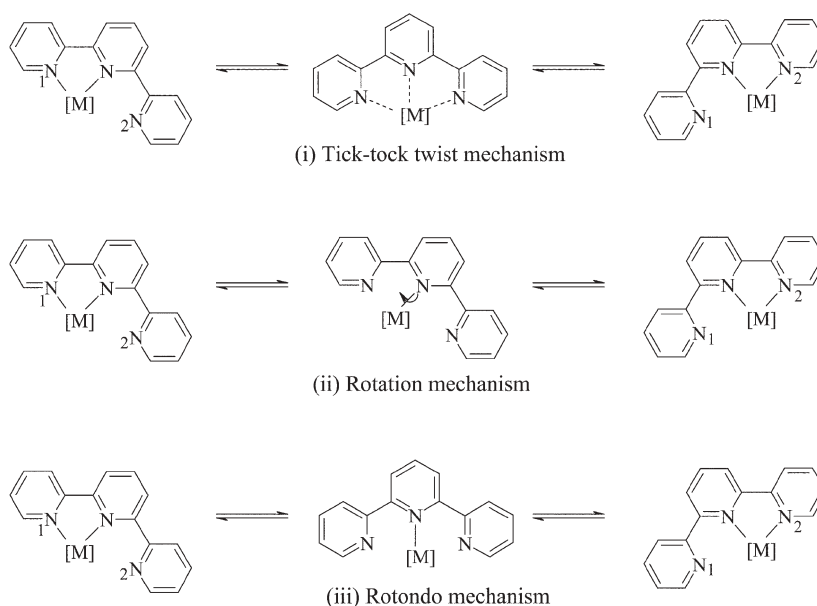
Hemilabile ligands with redundant donor atoms

If the bonding mode of a polydentate ligand is somehow restricted so that one or more of the donor atoms remains

un-coordinated, the resultant complexes are potentially fluxional. This type of fluxionality is exemplified by complexes of 2,2':6',2''-terpyridine (terpy) in which terpy is restricted to a bidentate bonding mode. Exchange occurs between pendant and co-ordinated pyridyl rings (Scheme 7).^{27,28}

The two possible mechanisms [(i) and (ii), Scheme 7] initially proposed for this process²⁷ are distinguishable by virtue of their different effects on the *trans* terpy auxiliary ligands on the metal centre. The 'tick-tock' pathway [mechanism (i), Scheme 7] leads to an averaging of the *trans* ligands, while the 'rotational' pathway [mechanism (ii), Scheme 7] does not. Detailed dynamic NMR studies on the [PtMe₃X(terpy)] (X = Cl, Br or I)²⁷ complexes and [Pd(C₆F₅)(terpy)]²⁹ provided strong evidence for the tick-tock pathway. The (*trans* terpy) equatorial ligands are exchanged at the same rate as the pendant and co-ordinated pyridyl rings. On examining the effect of pH on the rate of exchange in the [M(C₆F₅)(terpy)] (M = Pd or Pt) complexes, Rotondo *et al.*³⁰ concluded that the rate limiting step involved cleavage of the outer M–N(pyridyl) bond followed by the formation of a T-shaped intermediate, in which terpy is bound to the metal in a monodentate fashion *via* the central pyridyl N atom [mechanism (iii), Scheme 7]. This latter interpretation is supported, at least in part, by kinetic studies which indicate a dissociative ligand substitution pathway in some Pt^{II} sulfide complexes.³¹

Substitution of terpy in the octahedral complexes *fac*-[ReX(CO)₃(terpy)] with the analogous C₂-symmetric chiral, non-racemic ligand 2,6-bis[4-(*S*)-methyloxazolin-2-yl]pyridine (Mepybox) provides a more detailed spectroscopic handle on the stereodynamics, enabling all three proposed mechanisms to be distinguished unambiguously. Co-ordination of Mepybox to the [ReX(CO)₃] moieties also renders the metal centre chiral, giving rise to two pairs of diastereoisomers (Fig. 2).³² Of the six possible rate processes shown in Fig. 2 three are unique [k_1 (= k_6); k_2 (= k_5); k_3 (= k_4)] and are distinguishable by virtue of their different effects on the NMR line shapes in the



Scheme 7 Proposed mechanism for the exchange of pendant and co-ordinated pyridyl rings in bidentate terpy complexes.

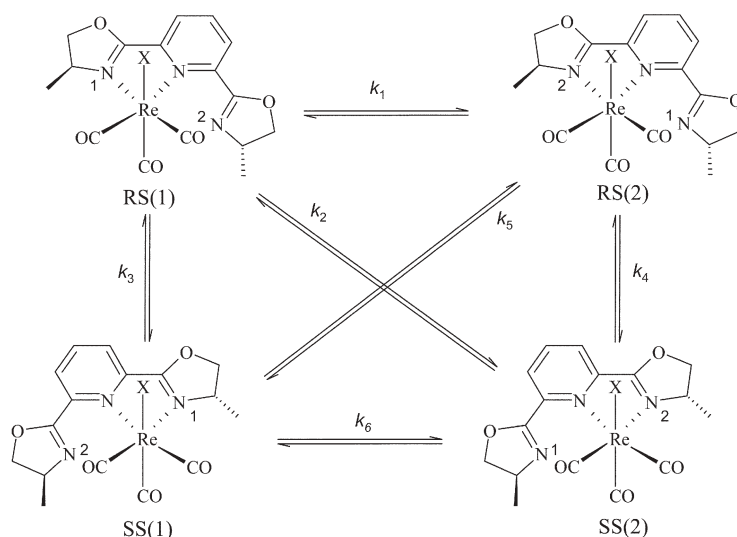


Fig. 2 The pairs of diastereoisomers of the $[\text{ReX}(\text{CO})_3(\text{Mepybox})]$ complexes and their interconversion pathways. The letters refer to the absolute configuration at the metal and the chiral carbon atom of the coordinated oxazoline ring, respectively. The numbers refer to which oxazoline ring is co-ordinated.

intermediate exchange regime. Rate process k_1 ($= k_6$) corresponds to the rotation mechanism. Rate process k_3 ($= k_4$) can arise from the tick-tock and/or Rotondo mechanisms, but it is possible to differentiate between the two. If free rotation about the M–N bond in the T-shaped intermediate of mechanism (iii) (Scheme 7) is rapid, as would be expected at the elevated temperatures at which the fluxional processes occur in these complexes (and indeed is required for the rotation mechanism, see below), then this pathway will also give a non-zero k_2 (k_5). The tick-tock pathway does not contribute to k_2 (k_5). The NMR line shapes could only be simulated on the basis of two, *independent* rate constants, namely k_1 (k_6) and k_3 (k_4).³² This shows clearly that both the tick-tock and rotations pathways are occurring independently, but that any contribution to the stereodynamics from the Rotondo pathway is negligible. The Gibbs free energies of activation for the two processes are given in Table 3, along with those for directly analogous dynamic processes in similar chiral complexes.^{32–38}

The same type of fluxional behaviour is observed in the chiral at phosphorus bis(oxazolinyl)phenylphosponite (NOPON) palladium(II) complexes $[\text{PdXY}(\text{NOPON})]$ (X, Y = uninegative ligands) and $[\text{Pd}(\eta^3\text{-allyl})(\text{NOPON})]$ (Fig. 3).³⁴ Although there is no direct mechanistic evidence, the effects of different auxiliary ligands, X and Y, on the exchange kinetics point clearly to a tick-tock pathway.

The fluxionality exhibited by the oxazolinyl complexes discussed above is not limited to purely N donor ligands. Analogous processes also occur in complexes with mixed donor sets, such as the bis(acetal)pyridine (O,N,O) ligands depicted in Fig. 4.^{35–38} Although no evidence has been found to indicate that the O atoms of the oxazolinyl ligands can co-ordinate, the bis(acetal) ligands form stable O,N bidentate complexes with the tricarbonylrhenium(I) halides, namely *fac*- $[\text{ReX}(\text{CO})_3(\text{O,N,O})]$, in which the Re–O bonds appear to be of comparable strength to the Re–N bonds in the oxazolinyl complexes (see below).^{35,36}

Co-ordination of the potentially terdentate chiral acetal ligands in a bidentate fashion renders both the metal centre and the acetal carbon atom of the co-ordinated acetal ring

Table 3 Free energies of activation^a for the exchange of co-ordinated and pendant donor groups in bidentate complexes of chiral terdentate ligands

Complex ^b	Mechanism ^c	$\Delta G^\ddagger/\text{kJ mol}^{-1}$	Reference
$[\text{ReCl}(\text{CO})_3(\text{Mepybox})]$	Tick-tock twist	74.5	29
	Rotation	83.9	29
$[\text{ReBr}(\text{CO})_3(\text{Mepybox})]$	Tick-tock twist	74.7	29
	Rotation	79.1	29
$[\text{ReI}(\text{CO})_3(\text{Mepybox})]$	Tick-tock twist	73.6	29
	Rotation	89	29
$[\text{W}(\text{CO})_4(\text{Mepybox})]$	Tick-tock twist	62.7	30
$[\text{Mo}(\text{CO})_4(^i\text{Prpybox})]$	Tick-tock twist	52.0	30
$[\text{W}(\text{CO})_4(^i\text{Prpybox})]$	Tick-tock twist	62.7	30
$[\text{ReCl}(\text{CO})_3(^i\text{Prpybox})]$	Tick-tock twist	79.0	30
$[\text{ReBr}(\text{CO})_3(^i\text{Prpybox})]$	Tick-tock twist	80.3	30
$[\text{ReI}(\text{CO})_3(^i\text{Prpybox})]$	Tick-tock twist	79.8	30
$[\text{PdI}_2(\text{NOPON})]$	Tick-tock twist	42 ($T_c = 227 \text{ K}$)	31
$[\text{Pd}(\eta^3\text{-allyl})(\text{NOPON})]$	Tick-tock twist	38 ($T_c \approx 200 \text{ K}$)	31
$[\text{ReCl}(\text{CO})_3(\text{O,N,O-1})]$	Tick-tock twist	72.3	32
	Rotation	83.3	32
$[\text{ReBr}(\text{CO})_3(\text{O,N,O-1})]$	Tick-tock twist	72.5	32
	Rotation	88.1	32
$[\text{ReI}(\text{CO})_3(\text{O,N,O-1})]$	Tick-tock twist	72.9	32
	Rotation	90.0	32
$[\text{ReCl}(\text{CO})_3(\text{O,NO,-2})]$	Tick-tock twist	79 ($T_1 = 318 \text{ K}$)	33
$[\text{ReBr}(\text{CO})_3(\text{O,N,O-2})]$	Tick-tock twist	72.3 ($T_1 = 323 \text{ K}$)	33
$[\text{ReI}(\text{CO})_3(\text{O,N,O-2})]$	Tick-tock twist	72.3 ($T_1 = 313 \text{ K}$)	33
$[\text{Rh}(\text{COD})(\text{O,P,N})]$	^d	46 ($T_c 243 \text{ K}$)	37
$[\text{Rh}(\text{COD})(\text{N,P,P,N})]$	^d	62.8	36

^a Free energies of activation quoted at 298 K unless otherwise specified. ^b Ligand abbreviations: Mepybox = 2,6-bis[4-(*S*)-methyl-oxazolin-2-yl]pyridine; ⁱPrpybox = 2,6-bis[4-(*S*)-isopropyl-oxazolin-2-yl]pyridine; NOPON = bis(2-oxazolin-4,4-dimethyl-2-hydroxydimethylphenylphosphite); O,N,O-1 = 2,6-bis[(4*R*,5*R*)-4,5-dimethyl-1,3-dioxolan-2-yl]pyridine; O,N,O-2 = 2,6-bis[(4*R*,6*R*)-4,6-dimethyl-1,3-dioxan-2-yl]pyridine; O,P,N = 6-[(2-methoxyphenyl)-(*S*)-phenylphosphanyl]-6-methylpyridine; N,P,P,N = *meso*- $[\text{Ph}_2\text{PCH}(\text{C}_5\text{H}_5)\text{N}]\text{CH}(\text{C}_5\text{H}_5)\text{NPPH}_2$. ^c See Scheme 7 for mechanisms. ^d See text for mechanism.

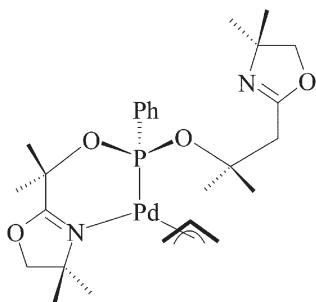


Fig. 3 Structure of $[\text{Pd}(\eta^3\text{-allyl})(\text{NOPON})]$. NOPON = bis(2-oxazoline-4,4-dimethyl-2-hydroxydimethyl)phenylphosphite.

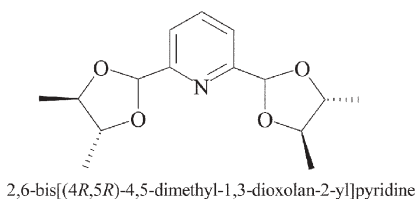
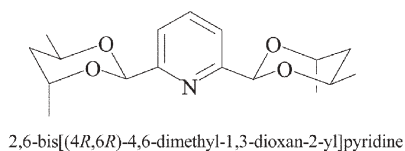


Fig. 4 2,6-Bis(acetal)pyridine ligands.

chiral, giving up to four possible diastereoisomers in solution (ignoring the stereogenic centres on the acetal rings, which are fixed). These are shown in Fig. 5. Above ambient temperature, the diastereoisomers undergo reversible dynamic interconversions characteristic of three independent fluxional processes, namely (i) a *flip* of the co-ordinated acetal ring (see below), (ii) exchange of co-ordinated and pendant acetal rings *via* a

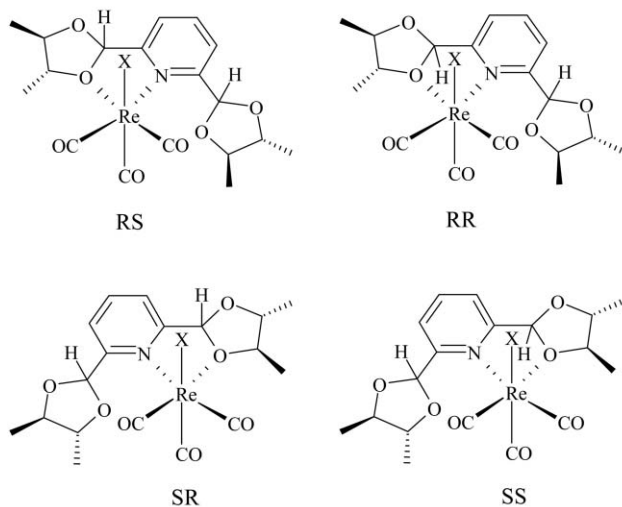


Fig. 5 The four possible diastereoisomers of the bis(dioxolanyl)pyridine complexes. The bis(dioxanyl)pyridine complexes are exactly analogous. Letters refer to the absolute configuration at the metal and the acetal-carbon atom, respectively.

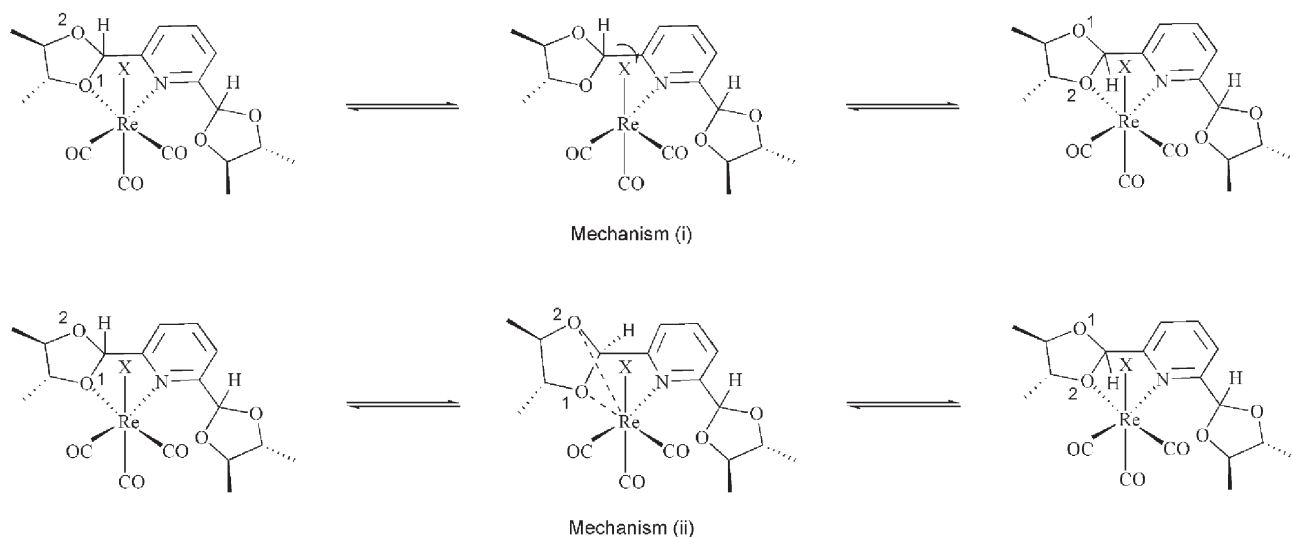
tick-tock pathway and (iii) exchange of co-ordinated and pendant acetal rings *via* a rotation pathway. Exchange of the co-ordinated and pendant acetal rings *via* both the tick-tock and rotation pathways can occur with either retention and/or inversion of configuration at the acetal carbon atom. While the observed magnetisation transfers show clearly that exchange occurs with formal retention of stereochemistry in the case of the rotation pathway, it was not possible to determine the effect of the tick-tock exchange mechanism on the configuration at the acetal carbon atom.

The free energies of activation for the tick-tock and rotation exchange pathways in the bis(acetal) complexes are reported in Table 3. Examination of Table 3 shows that the free energies of activation are of similar orders of magnitude for acetal and oxazolonyl complexes. This may be somewhat surprising given that the N donor of the oxazolonyl ring would be expected to be more nucleophilic and hence form stronger bonds with the metal (Re^{I}). In this context it would be of interest to compare the binding preferences of mixed 2-(acetal)-6-(oxazolonyl)pyridine ligands: work on this is currently underway in our laboratories.

The size of the acetal ring (5- or 6-membered) has a small, but distinct effect on the energetics of the tick-tock exchange. Despite the fact that calculations show dioxolanyl (5-membered acetal) co-ordination is favoured over dioxanyl co-ordination,³⁷ the free energies of activation are higher in the bis(dioxanyl) complexes. This presumably arises because the transition state, in which the ligand adopts a quasi terdentate co-ordination mode, is significantly more destabilised in the bis(dioxanyl) complexes. The underlying reasons for this are not clear.

Loosening of the Re–O bond followed by rotation about the acetal C–C(pyridyl) bond and subsequent binding of the second oxygen atom leads to a *flip* of the co-ordinated acetal ring.³⁵ The ring flip process leads to formal inversion of configuration at the acetal C atom and is readily distinguished from the other fluxional processes. This ring flip is also observed in tricarbonylrhenium(I) complexes of the chiral mono(acetal) (O,N) ligands, 2-(dioxolanyl)pyridine and 2-(dioxanal)pyridine, namely $[\text{ReX}(\text{CO})_3(\text{O,N})]$.^{35,38} The mechanism has not been established unambiguously but the low entropies of activation coupled with the fact that the flip is independent of, and has a lower activation energy than, the rotational exchange of the pendant and co-ordinated acetal rings in the $[\text{ReX}(\text{CO})_3(\text{O,N,O})]$ complexes tends to point to a more associated transition state, such as that in mechanism (ii), Scheme 8.

The rhodium(I) cyclooctadiene (COD) complex (Fig. 6) of the chiral N,P,P,N diphosphine ligand is a particularly interesting case.³⁹ The presence (or otherwise) of fluxionality depends on the absolute configuration of the ligand. With the exception of the *meso* isomer, the pyridyl groups adopt an equatorial/equatorial arrangement on ligand co-ordination and cannot interact with the metal centre. The Rh atom is thus four-coordinate, with the ligand acting in a bidentate P,P fashion. In the *meso* isomer the pyridyl groups adopt an axial/equatorial arrangement and can interact. In this case the Rh atom is five-coordinate, with one of the pyridyl rings occupying the fifth (axial) co-ordination site. Above ambient



Scheme 8 Possible mechanisms for the flip of the co-ordinated acetal ring in the (dioxolanyl)pyridine complexes. The (dioxanyl)pyridine complexes are exactly analogous.

temperature the pendant and co-ordinated pyridyl ligands exchange with a free energy of activation of *ca.* 63 kJ mol⁻¹.

Possible mechanisms for the exchange were not proposed by the authors³⁹ but, as with the fluxional processes discussed above, two extreme pathways may be envisaged, namely (i) an ‘associative’ mechanism in which the ligand adopts a quasi tetradentate bonding mode in the transition state or (ii) a ‘dissociative’ mechanism in which the ligand adopts a bidentate bonding mode in the transition state. Both pathways appear viable. On the one hand, it is (sterically) possible for both pyridyls to interact simultaneously with the metal while, on the other, bidentate P,P co-ordination is clearly not unfavourable. Measurement of the ¹J_{RhP} couplings in the fast exchange limit might allow the two mechanisms to be distinguished. The ¹J_{RhP} couplings are *ca.* 13 Hz higher in the bidentate (P,P only) complexes, indicating stronger Rh–P bonding. Any increase in the ¹J_{RhP} couplings in the fast exchange limit might therefore indicate an increase in the Rh–P bond strength concomitant with the formation of a bidentate intermediate (or *vice versa*).

The examples discussed so far all involve exchange between the same types of atom, namely N,N or O,O. In the rhodium(I) COD complexes of 2-[(2-methoxyphenyl)phenylphosphanyl]methyl]-6-methylpyridine N,O exchange occurs, with a free energy of activation of *ca.* 46 kJ mol⁻¹ (*T_c* = 243 K).⁴⁰ At ambient temperature a single doublet (¹J_{RhP} = 149 Hz) is observed in the ³¹P NMR spectrum. On cooling, this signal

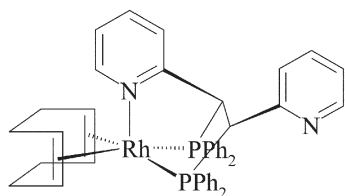


Fig. 6 Structure of [Rh(COD)(N,P,P,N)]. N,P,P,N = *meso*-[Ph₂PCH(C₅H₅N)CH(C₅H₅N)PPh₂].

resolves into two doublets in a 3 : 2 ratio, owing to the presence of both P,N and P,O bidentate co-ordination modes of the ligand: the major isomer was assigned as that with the ligand P,N co-ordinated. Although the P,O co-ordination mode might be expected to be of much higher energy and therefore unobservable in the NMR spectrum, a large steric interaction between the pyridyl methyl substituent and the metal moiety is thought to raise the ground state energy of the P,N chelate towards that of the P,O arrangement. The relatively high Rh–P coupling constant (see above) in the fast exchange regime points to a relatively strong Rh–P bond, possibly indicating a dissociative pathway with a monodentate bound intermediate.

Another example of exchange between different types of donor atoms has been reported in sulfonimidoyl-substituted η¹-allyltitanium(IV) complexes.⁴¹ These complexes are of particular interest because they are efficient reagents for the enantioselective allylation of aldehydes and they have been the subject of a very detailed study.⁴¹ Although the ambient temperature ¹H NMR spectra of the complexes indicate the presence of a single species, the patterns of reactivity suggest otherwise, and on cooling to *ca.* 213 K three distinct sets of signals are observed. The three sets of signals were assigned to species (a), (b) and (c) in Fig. 7. Species (a) is the dominant isomer when the allyl substituent, R, is *trans* to the Ti moiety, while (b) is the dominant isomer when R is *cis* to the Ti moiety.

The Ti atoms are formally tetra-coordinated, possessing a vacant co-ordination site that, in the C-bonded species [(a) and (c), Fig. 7], can be occupied by the N atom of the sulfonimidoyl group. These species are thus nicely set up to undergo facile 1,3-M,N metallotropic shifts, interconverting them with the N-titanium allyl ylide, (b), and leading to epimerisation of carbon atom C(1). This fluxional behaviour accounts for both the regio- and diastereo-selectivities observed for the aldehyde allylations.⁴¹

The corresponding 1,1-dialkyl complex (Fig. 8) is also fluxional, undergoing analogous 1,3-M,N shifts.⁴¹ The mechanism is thought to be similar to that proposed for the allyltitanium complexes, but a reversible β-hydride elimination

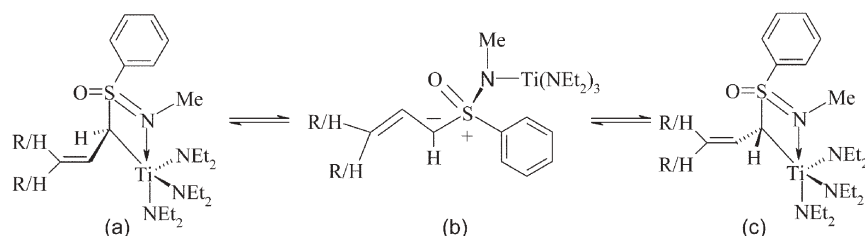


Fig. 7 Solution state species of the sulfonimidoyl-substituted η^1 -allyltitanium(IV) complexes and their possible interconversion pathways.

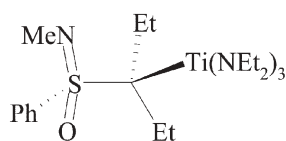


Fig. 8 The alkyltitanium complex (*R*)-tris(*N*-diethylaninato)-[3-(*N*-methyl-*S*-phenylsulfonimidoyl)-3-pentyl]titanium(IV).

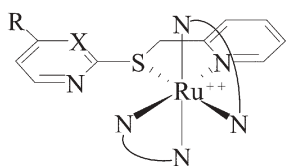


Fig. 9 Fluxional ruthenium bis(imine) complexes. N N = imine; X = CH or N; R = H or Me.

step must also be invoked to account fully for line shape changes that occur in the ^1H NMR spectra.

The interconversion of the potentially terdentate N,S,N ligands 2-(pyridin-2-ylmethylsulfanyl)pyridine and 4-methyl-2-(pyridin-2-ylmethylsulfanyl)pyrimidine between bidentate S,N(pyridyl) and monodentate N(pyridyl) modes in the octahedral cationic ruthenium(II) complexes shown in Fig. 9 has been reported to occur *via* a bidentate N,N bound intermediate.⁴² The formation of the N,N bound intermediate requires a 1,3-metallotropic shift with, presumably, a quasi terdentate bonding mode for the ligand in the transition state. This seems unlikely given the highly congested Ru centre and the fact that the free energies of activation are apparently independent of the ligand involved. Indeed it would seem more likely that the monodentate (N-bonded) species would be an intermediate in the formation of any N,N bound species (although no such species are observed in the NMR). Thus, here, the S donor atom is probably acting in a simple on/off fashion with no clear involvement of the pendant donor atom in the fluxional process.

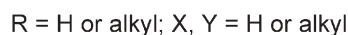
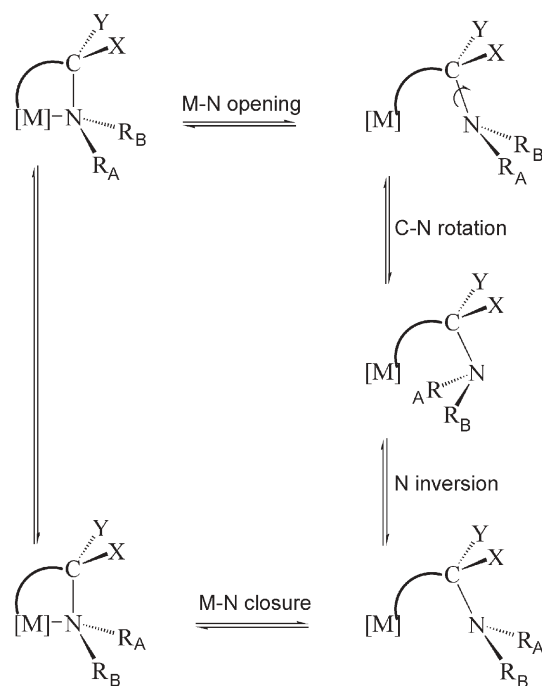
Hemilabile ligands without redundant donor atoms

The reversible opening and closure of metal-donor atom bonds, exemplified by the on/off co-ordination of the S atom suggested in the Ru N,S,N complexes (above), is a common feature of hybrid hemilabile ligand complexes, particularly those involving an amine group as one of the functionalities. Such processes are often only observable in chiral compounds. The free energy of activation for metal–N bond opening is significantly greater than that of N inversion or C–N bond

rotation. Thus in the open configuration N inversion and rotation about the C–N(R₂) bond occurs freely, leading to exchange of the N–R environments on closure of the M–N bond, as shown in Scheme 9. The exchange of the N-substituents is readily observable in chiral complexes because they are diastereotopic, giving rise to two separate signals in the slow exchange limit.

In cases where the metal is chiral the exchange of the diastereotopic N-substituents could also be brought about by inversion of configuration at the metal centre. Although inversion at the metal centre and the opening of the M–N bond give rise to exactly the same effect on the N–R NMR signals, they are distinguishable because inversion at the metal also leads to exchange of environments on the ligand backbone, whereas opening of the M–N bond followed by inversion/rotation and re-coordination does not.

There are many examples of M–N bond opening fluxional processes in both main group and transition metal complexes. In complexes of main group elements and the Zn triad, such



Scheme 9 Exchange of N-substituents in hemilabile amine complexes. The rate determining step is M–N bond rupture.

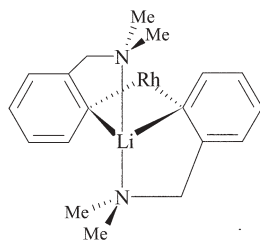


Fig. 10 Heterobimetallic Li/Rh complexes with chelating arylamine ligands. Rhodium is also co-ordinated to cyclooctatadiene, which has been omitted for clarity. The *ipso* carbon atoms of the two arylamine ligands are chiral, possessing the same absolute configuration.

processes have been studied largely in complexes of C,N ligands.^{43–49}

In the heterobimetallic Li/Rh complex shown in Fig. 10⁴⁸ the two, bridging *ipso* carbons are chiral. The dimeric structure requires that both carbons possess the same absolute configuration. At 213 K, the ¹H NMR spectrum displays two singlets and two doublets due to the diastereotopic NMe₂ and benzylic –CH₂– groups, respectively. On warming, the *N*-methyl signals broaden, coalesce (at *ca.* 230 K) and then sharpen again to give a single time-averaged signal. Importantly, the AB spin system of the benzylic group remains unaltered (at least up to 380 K). This latter observation excludes the possibility of racemisation occurring at the *ipso* carbon atoms. Variable temperature ¹H NMR data are thus consistent with the reversible co-ordination of the lithium bound amino groups. The free energy of activation estimated from the low temperature limiting spectrum is *ca.* 45–50 kJ mol^{–1}.

An exactly analogous process is observed in the chiral hypervalent Bi complexes [BiCl{2-(Me₂NCH₂)C₆H₄}{Ph₂P(E)NP(E)Ph₂}] (E = S or Se).⁴⁵ The free energy of activation is ≈ 62 kJ mol^{–1} (at *T_c* = 298 K) and is essentially independent of the chalcogen atom, E (E = S or Se). The AB pattern of the benzylic hydrogens remains unaffected (in CDCl₃) over the temperature range studied, indicating the configuration stability of the Bi atom. A second, independent fluxional process is observed in the ³¹P NMR. Two doublets (²*J*_{PP} = 7–8 Hz), owing to the two different phosphorus environments, are observed in the low temperature limiting spectrum (228 K), which coalesce to a singlet on warming. The activation energy is, again, apparently independent of the chalcogen, E: $\Delta G^\ddagger(T_c) \approx 57$ kJ mol^{–1}. Rather than being brought about by the reversible cleavage of the Bi–N bond, the exchange of the phosphorus environments presumably results from cleavage of

one of the Bi–P atoms, as shown in Scheme 10. Thus the Ph₂P(E)NP(E)Ph₂ ligand can also be considered as a hemilabile ligand. In this case, the hemilability is presumably brought about by the relative *trans* influences of the N and Cl ligands.

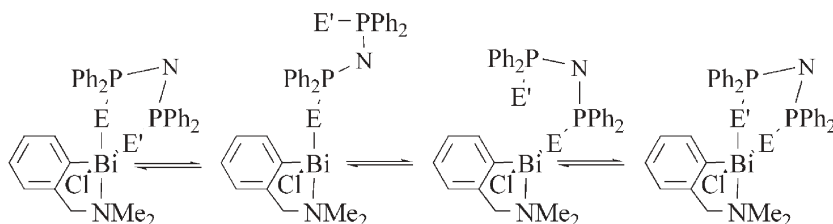
The barrier to inversion at Bi (see above) is greatly diminished in co-ordinating solvents and at 298 K in DMSO only one averaged signal is observed for the benzylic hydrogen atoms. This exchange of benzylic hydrogen environments results from inversion of configuration at Bi, which is thought to occur *via* a solvent-assisted *edge* mechanism, which also requires opening of the P,P chelate.

Toyota *et al.*^{43,44} have reported that exchange of the NMe groups in the boron complexes [BXPh(C₆H₄CH₂NMe₂)] (X = anionic donor ligand, such as OC(O)CF₃, Cl or Me) occurs at approximately the same rate as inversion of configuration at boron, at least in the X = OC(O)CF₃ complex. Inversion at boron is thus presumed to result from rotation about the B–C(aryl) bond in the (B–N) open configuration. The free energies of activation of NMe exchange, which are in the range 95–108 kJ mol^{–1}, are dependant on the Lewis acidity of the boron centre: the more Lewis acidic, the higher the barrier. Where X = OC(O)C₂F₅ the barrier to inversion is sufficiently high to enable the enantiomers to be separated by chiral HPLC.⁴³

In the diorganylboron complexes of ephedrine and pseudoephedrine reversible B–N bond cleavage occurs with a free energy of activation in the narrow range *ca.* 65–71 kJ mol^{–1}.⁵⁰ ΔG^\ddagger is *ca.* 3 kJ mol^{–1} higher in the pseudoephedrine complexes, indicating a slightly stronger B–N bond. This dependence presumably arises because reduced steric interactions lead to a more stable BON chelate in the pseudoephedrine complexes.

In all cases mentioned above, the *N*-alkyl substituents are exchanged by rapid inversion at N followed by C–N bond rotation in the ‘open’ configuration of the complexes, irrespective of any other fluxional processes occurring. Although the N substituents clearly cannot be exchanged in a directly analogous process in the *N-spiro*-like boron complexes depicted in Fig. 11,⁵¹ dynamic NMR studies have shown that the diastereotopic B-phenyl groups are exchanged. The observed exchange results from opening of the B–N bond followed by B–O rotation {*cf.* racemisation of boron in [BXPh(C₆H₄CH₂NMe₂)]}.

The free energies of activation for these B–N bond opening processes are given in Table 4. As might be expected, examination of Table 4 reveals a *general* trend of increasing activation energy with decreasing B–N bond length. Table 4



Scheme 10 Proposed mechanism for the exchange of phosphorus environments in [BiCl{2-(Me₂NCH₂)C₆H₄}{Ph₂P(E)NP(E)Ph₂}] (E, E' = S or Se).

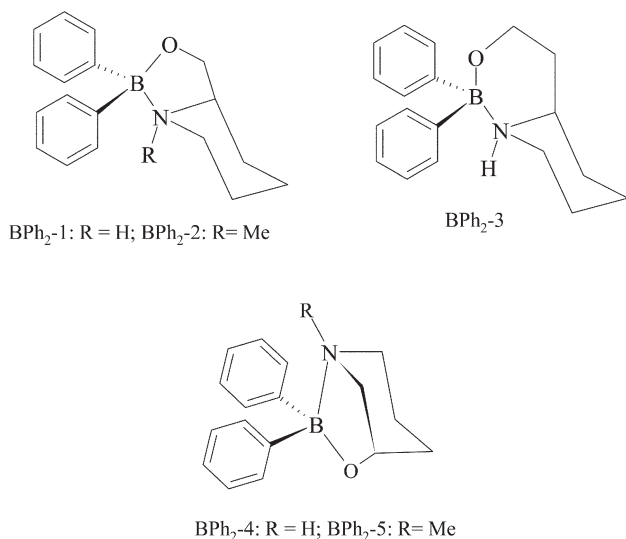


Fig. 11 *N*-spiro-like borinate complexes. The abbreviations (BPh₂-1 etc.) refer to those used in Table 4.

also reveals that, in the *N*-spiro-like compounds, the free energies of activation are greater in the six-membered chelates than in the five-membered. This increase arises presumably because there is less strain in the six-membered chelates, allowing the formation of a measurably stronger B–N bond (this can also be seen in the shorter B–N bond lengths). The reasons for the significantly lower free energies of activation (up to *ca.* 50 kJ mol⁻¹) for B–N bond cleavage in the N,O chelates compared to the C,N chelates have not been explored,

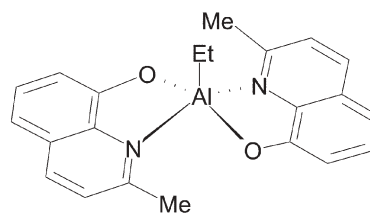


Fig. 12 Structure of [AlEt(2-MeOx)₂]. Racemisation of the metal centre is presumed to occur by simultaneous rotation of the two quinolate ligands, which may be initiated by opening of the Al–N bonds.

but may result from stabilisation of the three co-ordinate intermediate as a result of ππ–ππ overlap between filled orbitals on the O and the vacant orbital on B.

Reversible opening of the M–N bonds is also thought to give rise to the Λ, Δ racemisation observed in the six-coordinate [Zr(N,O,O)₂]⁵² and [MR₂(Ox)₂]⁵³ complexes {N,O,O = bis(alkoxide)amine; M = Zr or Hf, Ox = a quinolate} and probably accounts for the five-coordinate rearrangements in [ZrR₂(N,O,O)]⁵⁴ and [Al(Et)(2-MeOx)₂] (2-MeOx = 2-methyl-8-quinolato) (Fig. 12).⁵⁵ The free energies of activation for the Zr and Hf complexes, which lie in the range 63–73 kJ mol⁻¹, decrease with increasing steric bulk around the nitrogen atom, consistent with a weakening of the M–N bond in the ground state. The free energy of activation in [Al(Et)(2-MeOx)₂] is *ca.* 79 kJ mol⁻¹ at 298 K.

Despite the fact that the tris(phenoxide)amine ligands adopt a chiral propeller arrangement in the five-coordinate silicon⁵⁶ and phosphorus^{57–59} [MR{tris(phenoxide)amine}]

Table 4 Gibbs free energies of activation for M–N bond opening and M–N bond distances in main group complexes of hemilabile amine ligands^a

Complex	ΔG [‡] /kJ mol ⁻¹	M–N distance/Å	Reference
[Rh(COD)(μ-L-1) ₂ Li] ^b	45–50 (213 K)		48
[BPh(L-1){OC(O)CF ₃ }]	108 (408 K)		43,44
	112 (346 K)		
[BPh(L-1){OC(O)CF ₂ CF ₃ }]	116 (356 K)	1.668	43,44
	121 (298 K)		
[BClPh(L-1)]	112 (408 K)	1.667	44
[BMePh(L-1)]	103 (413 K)	1.706	44
[BFPh(L-1)]	94 (393 K)		44
[BPh ₂ (L-2)]	68 ^c	1.66	50
[BPh ₂ (L-3)]	71 ^c	1.66	50
[BPh ₂ (L-4)]	65 ^c		50
[BPh ₂ (L-5)]	68 ^c	1.66	50
[BPh ₂ (L-6)]	50 ^c	1.745	50
[BPh ₂ (L-7)]	53 ^c	1.74	50
[BPh ₂ -1] ^d	55 (265 K)	1.648	51
[BPh ₂ -2] ^d	53 ^c	1.73	51
[BPh ₂ -3] ^d	58 ^c	1.673	51
[BPh ₂ -4] ^d	51 ^c		51
[BPh ₂ -5] ^d	59 ^c		51
[AlEt(L-8)]	71 (350 K)		55
[SiR{N(CH ₂ C ₆ H ₂ (CH ₃) ₂ O) ₃ }]	<i>ca.</i> 42 ^e	2.19–2.75	56
[Si(CCl ₃)N{CH ₂ C ₆ H ₂ (CH ₃) ₂ O} ₃]	>70	2.03	56,59
[PMeN{CH ₂ C ₆ H ₂ (CH ₃) ₂ O} ₃] ⁺	47 ^c		57
[BiCl(L-1)(S,S)]	61.5 (298 K)	2.554	45
[BiCl(L-1)(Se,Se)]	61.9 (298 K)	2.575	45

^a Ligand abbreviations: L-1 = 2-(Me₂NCH₂)C₆H₄-; L-2 = [1-(*R*)-phenyl-2-(*S*)-methyl-2-aminoethoxy]; L-3 = [1-(*R*)-phenyl-2-(*R*)-methyl-2-aminoethoxy]; L-4 = *N*-(*R*)-methyl-[1-(*R*)-phenyl-2-(*S*)-methyl-2-aminoethoxy]; L-5 = *N*-(*S*)-methyl-[1-(*R*)-phenyl-2-(*R*)-methyl-2-aminoethoxy]; L-6 = *N,N*-dimethyl-[1-(*R*)-phenyl-2-(*S*)-methyl-2-aminoethoxy]; L-7 = *N,N*-dimethyl-[1-(*R*)-phenyl-2-(*R*)-methyl-2-aminoethoxy]; L-8 = 2-methyl-8-quinolato; S,S = Ph₂P(S)N(S)PPh₂; Se,Se = Ph₂P(Se)N(Se)PPh₂. ^b Li–N bond opening. ^c Measured at coalescence temperature (temperature not reported). ^d See Fig. 11 for complex abbreviations. ^e Average value for various R substituents.

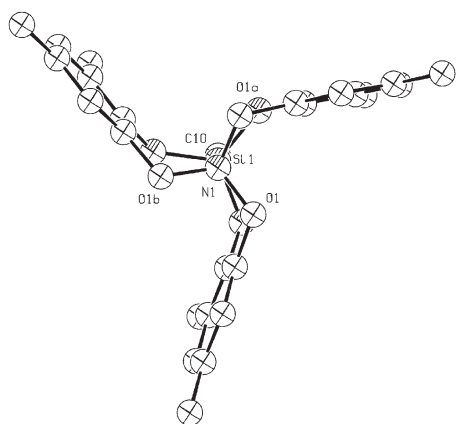
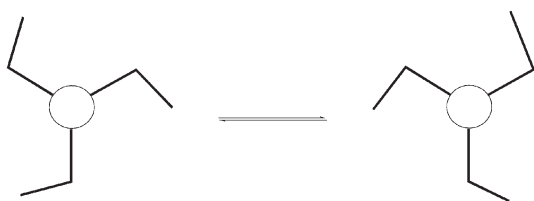


Fig. 13 ORTEP plot (arbitrary ellipsoid probability) of $[\text{SiMe}\{\text{N}\{(\text{C}_6\text{H}_2(\text{CH}_3)_2\text{O})_3\}]$, viewed down the N–Si–C axis showing the propeller configuration. Carbon atom labels omitted for clarity. Analogous propeller configurations are observed in the other tris(phenoxide)amine complexes.



Scheme 11 Racemisation of the chiral propeller configurations in complexes of tris(phenoxide)amine ligands.

(R = organic ligand) complexes (Fig. 13), a single NMR signal is observed for the diastereotopic methylene hydrogens at ambient temperature, indicating rapid racemisation of the two configurations (Scheme 11). The mechanism of this rearrangement is not known, but it has been suggested that a simultaneous *flip* of the phenyl rings, which may be initiated by the opening of the M–N bond, occurs.⁵⁶ Although the free energies of activation [*ca.* 42 kJ mol^{−1} (average) (Si) and 47 kJ mol^{−1} (P)] appear essentially independent of the M–N bond distances, it is noteworthy that the Si–CCl₃ derivative, which has a particularly short Si–N bond (2.03 Å), is configurationally stable.

The analogous five- and six-coordinate titanium(IV) complexes, $[\text{Ti}(\text{iOPr})(\text{L})]$ and $[\text{Ti}(\text{L},\text{O})(\text{L})]$ {L = tris(phenoxide)amine ligand; L,O = bidentate O,O or N,O ligand}⁶⁰ show identical behaviour. The free energies of activation for the six-coordinate complexes are in the range 36–48 kJ mol^{−1}, while that for the five-coordinate complex is *ca.* 75 kJ mol^{−1}. The

large rate enhancement in the six-coordinate complexes is attributed to an increase in steric crowding in the ground state. As in the main group complexes (above) the extent of any M–N bond loosening during the course of the dynamic process remains conjecture.

Among the transition metals complexes that possess fluxional hemilabile ligands, hybrid P/N ligands are particularly common: the M–P bond remains intact while the M–N bond displays reversible opening. Jalón and co-workers have studied the fluxionality displayed by Pd⁰ and Pd^{II} olefin complexes of chiral (aminoferrocenyl)phosphane ligands, such as PPFA, PAFP and PTFA (Fig. 14).^{61–64}

Two diastereoisomers are observed in a *ca.* 80 : 20 ratio in solutions of $[\text{Pd}(\eta^2\text{-dba})(\text{PAFP})]$ (dba = dibenzylidene-acetone).⁶² In the major isomer, dba is bonded in an *s-cis,trans* conformation *via* the *re*-face of the *trans* double bond, while in the minor species, it is co-ordinated *via* the *si*-face. On warming, exchange of the PAFP NMe signals is observed within each isomer as well as between the two isomers. The fluxional processes are unaffected by the addition of free dba (the free dba signals remain sharp throughout the temperature range), confirming that the exchanges are intramolecular. The observed band shape changes indicate a diastereo-isomerisation process, exchanging the *re*- and *si*-faces of dba, occurring simultaneously with reversible opening of the Pd–N bond. The free energy of activation for the diastereo-isomerisation is *ca.* 66 kJ mol^{−1} (³¹P NMR; *T*_c = 348 K). Two plausible mechanisms for the diastereo-isomerisation are shown in Scheme 12.⁶²

Only one isomer is observed in the corresponding PPFA complex, $[\text{Pd}(\eta^2\text{-dba})(\text{PPFA})]$, in which (in the solid-state) the dba ligand is again bound *via* the *re*-face of the *trans* double bond. As expected, reversible exchange of the aminomethyl signals is observed, owing to the hemilability of the PPFA ligand. The free energy of activation is 57 kJ mol^{−1} (*T*_c = 301 K).

The significantly higher activation energy for the PAFP analogue is in keeping with results reported by the same authors for other Pd olefin complexes (olefin = dimethylfumerate or maleic anhydride).^{63,64} The barrier to Pd–N opening is in the range 63–75 kJ mol^{−1} (at *T*_c) for the PPFA complexes, but lies above the (NMR) accessible magnitudes for the PAFP (and PTFA) complexes. The comparatively low value for ΔG^\ddagger in the $[\text{Pd}(\eta^2\text{-dba})(\text{PAFP})]$ complex probably arises because dba is a poor electron-acceptor. The greater electron density that results at the metal presumably allows for the formation of a weaker Pd–N interaction in the ground state. The reasons for the greater barriers in the less flexible

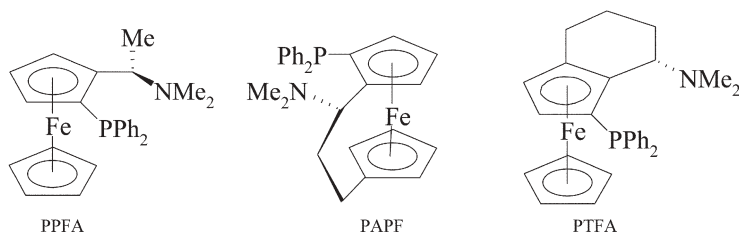
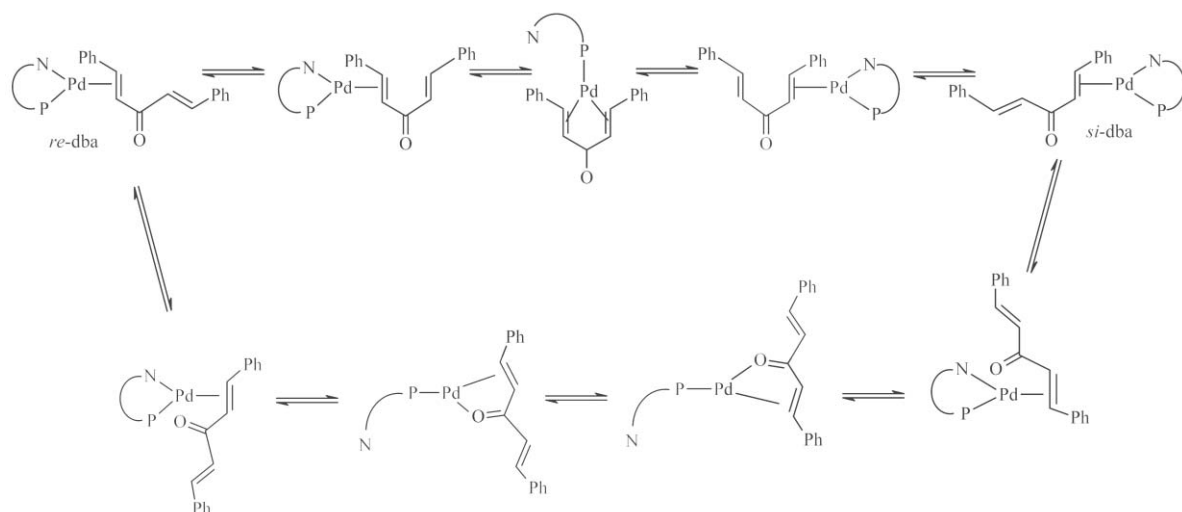


Fig. 14 The ferrocenyl aminophosphine ligands PPFA, PAFP and PTFA.



Scheme 12 Possible mechanisms for the diastereo-isomerisation of $[\text{Pd}(\eta^2\text{-dba})(\text{PAPF})]$.

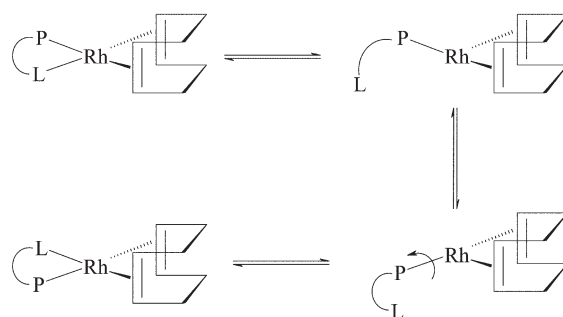
PAPF and PTFA complexes have not, as far as the author is aware, been investigated. Given the importance of these types of complex, for example as pre-catalysts for a variety of asymmetric organic transformations, further studies on the factors affecting the lability of the metal–N bond would be of interest.

The NMe signals in the mononuclear Pd^0 complex of the potentially terdentate P,P,N chiral ferrocenyl ligand, *N,N*-dimethyl-1-[2,1'-bis(diphenylphosphino)ferrocenyl]ethylamine (BPPFA), namely $[\text{Pd}(\text{DMFU})(\text{BPPFA})]$ (DMFU = dimethylfumerate), decoalesce on cooling, consistent with the formation of a static Pd–N bond on the NMR time-scale. Thus at low temperature, BPPFA appears to be acting in a $\kappa^3\text{-P,P,N}$ fashion, giving an unusual five-coordinate Pd^0 metal centres.†.‡ Identical behaviour is observed in the Pd^{II} $[\text{Pd}(\text{C}_6\text{F}_5)_2(\text{BPPFA})]$ and $[\text{PdClMe}(\text{BPPFA})]$ complexes, again suggesting a rather unusual five-coordinate metal centre at low temperature.⁶¹ However, in the case of $[\text{Pd}(\text{C}_6\text{F}_5)_2(\text{BPPFA})]$ the static NMR spectrum indicates the presence of two isomers, one P,P,N co-ordinated, the other (minor) with an open Pd–N configuration (*i.e.* $\kappa^2\text{-P,P}$ ligand bonding mode). The two isomers are interchanged by a mutual twist of the two Cp rings, with a free energy of activation of *ca.* 45–46 kJ mol^{-1} at 233 K.

Dynamic NMR studies on the $[\text{Rh}(\text{COD})(\text{P,L})]$ cationic complexes (P,L = chiral bidentate P,N or P,S donor ligand) clearly reveals the pair-wise exchange of olefinic hydrogen environments (Scheme 13). This could be attributed to ‘rotation’ of COD about the axis bisecting the rhodium diolefin angle, were it not for the fact that analogous complexes of bidentate diphosphine ligands do not exhibit the same structural dynamics.⁶⁵ The exchange of the olefinic COD resonances is thus attributed to a process analogous to the ‘Rotondo’ mechanism proposed for the exchange of the

outer pyridyl rings in the bidentate complexes of terpy (see above),³⁰ in which the Rh–N (or S) bond undergoes reversible cleavage, to form a T-shaped intermediate, as shown in Scheme 13. Similar mechanisms have been advanced to account for the dynamic behaviour observed in some late transition metal complexes of bidentate N,N donor ligands.^{66,67}

Hybrid N,O donor ligands represent another interesting class of fluxional hemilabile ligands. In complexes of anionic N,O ligands, in which the O atom carries the negative charge, the N atom is the labile donor, but in neutral amino ether or alcohol complexes the oxygen atom is the more labile. The $[\text{RuCl}_2\text{PPh}_3]$ complexes of chiral tripodal P,N,O ligand are interesting because the hemilabile behaviour depends on which donor atom (N or O) is *trans* to PPh_3 .⁶⁸ The complexes exist as a mixture of two isomers, which differ by the position of the PPh_3 ligand relative to the ether and pyridyl donor groups: PPh_3 is *trans* N in one isomer and *trans* O in the other. When the pyridyl donor is *trans* PPh_3 , reversible Ru–N bond rupture occurs. This is clearly demonstrated by the development of a $^3J_{\text{PH}}$ coupling between the triphenyl phosphine moiety and the α -hydrogens of the pyridyl ring on cooling to *ca.* 193 K. The situation is less clear in the second isomer (O *trans* PPh_3). On cooling to 193 K (the lowest temperature limit studied) little



Scheme 13 A Rotondo-type mechanism accounts for the exchange of the COD signals in the $[\text{Rh}(\text{COD})(\text{P,L})]$ (P,L = chiral bidentate P,N or P,S donor ligand).

† Although a Pd–N interaction is proposed in solution, it is noteworthy that there is no Pd–N interaction in the solid-state. The N lone pair is not oriented directly towards the Pd atom: Pd–N non-bond distance = 4.327 Å.

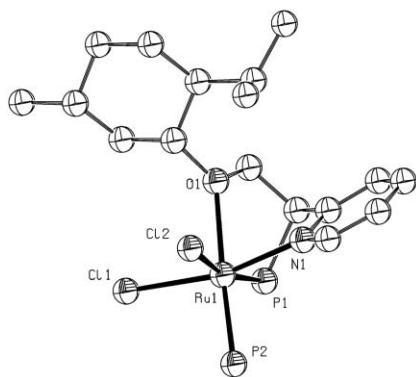


Fig. 15 ORTEP plot (arbitrary ellipsoid probability) of $[\text{RuCl}_2\text{-PPh}_3(\text{P,N,O})]$ {P,N,O = (*S*)-1-(diphenylphosphino)-2-[(1*R*,2*S*,5*R*)-methoxy]-1-(2-pyridyl)ethane}. In the isomer depicted, the O atom, which is *trans* P, exhibits reversible metal co-ordination. The *P*-phenyl groups and the C atom labels omitted for clarity.

change is observed in the NMR spectra. However, the X-ray molecular structure of this isomer (Fig. 15) reveals a long Ru–O bond (2.331 Å), suggesting a weak Ru–O interaction. The lack of any significant changes in the variable temperature NMR spectrum thus suggest Ru–O bond opening/closure remains rapid even at 193 K.

Reversible opening of M–O bonds has also been reported in some Lewis acidic early transition metal and lanthanide complexes of ligands containing alcohol,⁶⁹ amide⁷⁰ or ether^{71,72} functional groups. Such complexes are of interest because of their potential applications in organic synthesis.^{70,71}

The pseudo-tetrahedral chiral-at-metal Mo phenolate complex $[\text{Mo}\{\text{C}_7\text{H}_6\text{-C}_6\text{H}_2(\text{Me})_2\text{O}\}(\text{CO})(\text{PPh}_3)][\text{BF}_4]$ is static on the NMR time-scale at ambient temperature, but protonation of O gives the fluxional phenol analogue.⁶⁹ The weakening of the Mo–O bond that occurs on protonation, which facilitates the fluxional behaviour observed, is clearly revealed by the lengthening of the bonds in the solid-state: $\Delta(\text{Mo}-\text{O}) = 0.107 \text{ \AA}$.

Fluxional processes in polymetallic complexes of hemilabile ligands

Although the presence of additional metal centres opens up the possibility of an extended variety of ligand bonding modes (see Scheme 6 and reference 26), the fluxionality observed in polymetallic complexes of hemilabile ligands is generally directly analogous to that observed in mononuclear complexes.

Thus, for example, reversible opening of the non-bridging M–L (L = N or O) bond is observed in the type V (Scheme 6) lanthanide complexes $[\text{LnCp}'(\mu\text{-O,L})_2]$ (Cp' = η^5 -cyclopentadienyl ligand; O,L = chiral bidentate O,N or O,O ligand)^{73,74} in an exactly analogous fashion to that observed in the mononuclear amine and ether complexes discussed above.

Although, again, similar to some of the fluxional processes already mentioned, the dinuclear rhodium complex in Fig. 16 is noteworthy because (unusually) a diphosphine ligand is acting in a hemilabile fashion.⁷⁵ The P donor atom co-ordinated to the Rh(COD) moiety undergoes reversible cleavage, followed by rotation about the Rh(COD)Cl–Ru

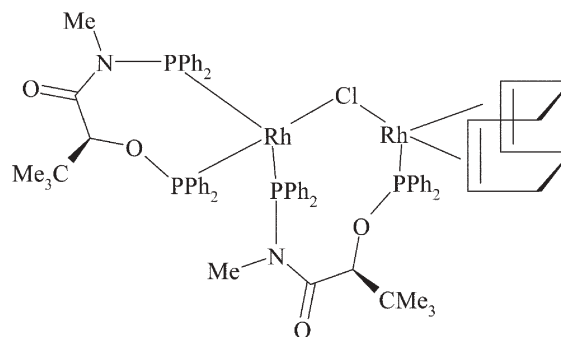


Fig. 16 Opening of the Rh(COD)–P bond in the above complex, followed by rotation about the Rh–Cl bonds then re-coordination of the P atom leads to exchange of the cyclooctadiene hydrogen environments.

bond: subsequent re-coordination leads to the averaging of the COD resonances in the NMR spectrum (*cf.* Scheme 13)

Alkyl lithium compounds, which are important organometallic reagents, exist as aggregates in solution. The degree of aggregation depends on several factors, such as solvent polarity, concentration and the size of the alkyl groups. Such aggregates are known to undergo various inter- and intramolecular rearrangements, as revealed by the temperature dependence of the $^1J_{\text{LiC}}$ scalar coupling constants.⁷⁶ However, the (usually) high symmetry of the aggregates has frustrated a detailed analysis of the structural dynamics. Breaking the symmetry by the introduction of a chiral Li unit, such as lithium (*S*)-2-(1-pyrrolidinylmethyl)pyrrolidie, Li-1, permits the site exchanges to be measured directly, as shown by the ^6Li - ^6Li 2D EXSY spectrum of tetrameric $(\text{Li-1})(^n\text{BuLi})_3$ (Fig. 17).⁷⁶ $(\text{Li-1})(^n\text{BuLi})_3$ exhibits a distorted cubane structure, with four inequivalent Li atoms. With the exception of Li(3) and Li(4) (Fig. 17), the cross-peaks between which probably result from a multi step process, it was reported that

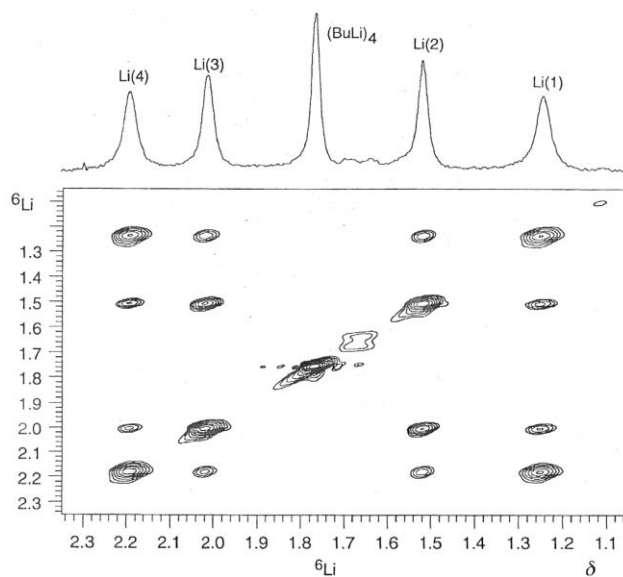


Fig. 17 Lithium-6 2D EXSY spectrum of $(\text{Li-1})(^n\text{BuLi})_3$, showing the Li site exchanges. (Reproduced by permission from reference 76. Copyright 1999 WILEY-VCH.)

a quantitative analysis of the 2D EXSY spectrum indicated that the Li atoms underwent a series of two-site exchanges at different rates. The exchange mechanism probably involves reversible cleavage of C–Li bonds along different edges of the ‘cube’. Such a mechanism also accounts for the observed racemisation of the stereogenic carbon centres in chiral organolithium reagents.⁷⁶

In the presence of (*S*)-2-(1-pyrrolidinylmethyl)pyrrolidine (1), Li-1 forms (Li-1)₂(1), which undergoes a rapid amine–amide interconversion *via* intramolecular proton transfer and exchange of the two (different) Li environments.⁷⁷ The free energies of activation are approximately equal (*ca.* 46 kJ mol^{−1}, measured at *T*_c), indicating that the two processes are strongly correlated.

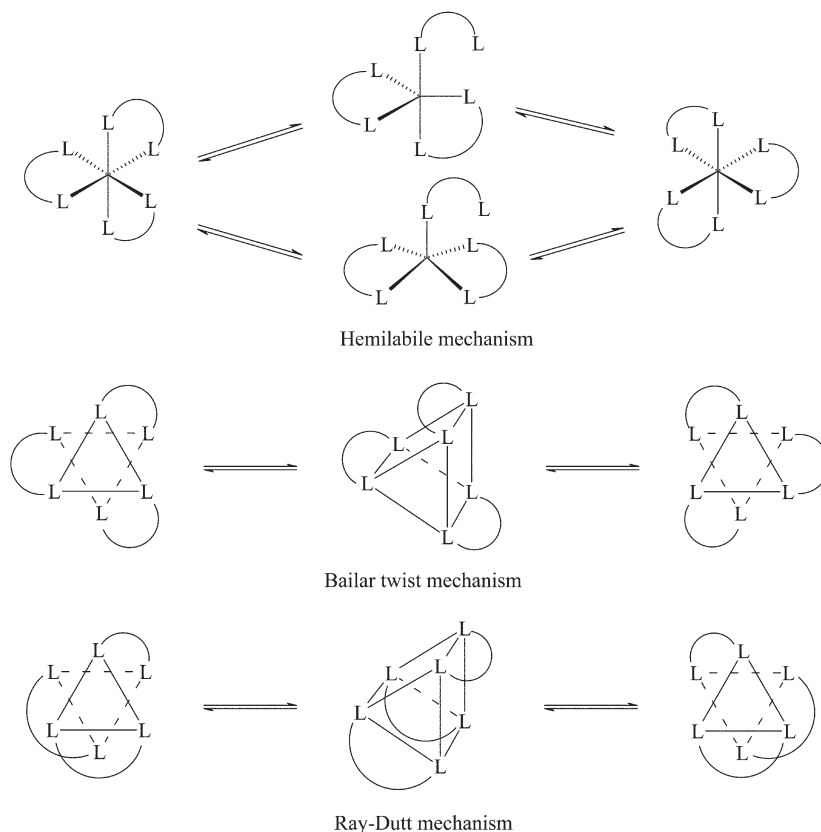
Fluxional complexes of non-labile ligands

Six-coordinate rearrangements

Racemisation between Λ and Δ forms has long been known to occur in octahedral tris(chelate) complexes. Three possible mechanisms that can account for this racemisation are depicted in Scheme 14. One possible mechanism involves reversible cleavage of one of the metal–ligand bonds (*i.e.* a hemilabile mechanism, *e.g.* see references 52–54 and 78), while the other two involve twisting around one of the pseudo C_3 axes of symmetry (see below). The twist mechanisms do not necessitate any bond breaking. The bond rupture mechanism can be distinguished from the twist mechanisms *via* solvent

effects on the exchange rate. Exchange rates increase with increasing solvent dielectric constant owing to greater solvation of the transition state. For example, in [Ga(tta)₃] (tta = 2-thenoyltrifluoroacetone) the rate of racemisation increases 10-fold on changing the solvent from (CDCl₂)₂ to d₆-DMSO.⁷⁸ Of the three possible intermediates that can be envisaged in the bond rupture mechanism, namely (i) a trigonal bipyramidal intermediate with a pendant equatorial ligand, (ii) a trigonal bipyramidal intermediate with a pendant axial ligand and (iii) a square pyramidal intermediate, only the latter two (depicted in Scheme 14) lead to racemisation.

The twist mechanisms differ in their transition-state symmetries and depend on the pseudo C_3 axis about which twisting occurs. The Bailar (trigonal) twist possesses pseudo D_{3h} transition-state symmetry, while the Rây–Dutt (rhombic) twist possesses a pseudo C_{2v} transition-state (Scheme 14). The two mechanisms can be distinguished in complexes of unsymmetrical chelate ligands that undergo both racemisation and isomerisation (*cis*, *trans*, *mer*, *fac*): isomerisation is only possible *via* the Rây–Dutt twist. Distinguishing between the twist mechanisms in complexes of symmetric ligands can be difficult because they usually produce similar band shape changes. Use of modern DNMR techniques, particularly 2D EXSY, has enabled the twist mechanisms to be studied more fully.^{78,79} In the slow exchange regime they can be distinguished by virtue of their different magnetisation transfers. Although each twist interchanges a pair of ligands three such twists, each of which permutes a different pair of ligands,



Scheme 14 Mechanisms of Δ , Λ racemisation in six-coordinate tris(chelate) complexes. Note, in the hemilabile mechanism, a trigonal bipyramidal intermediate with a pendant equatorial ligand (not shown) does not give rise to racemisation.

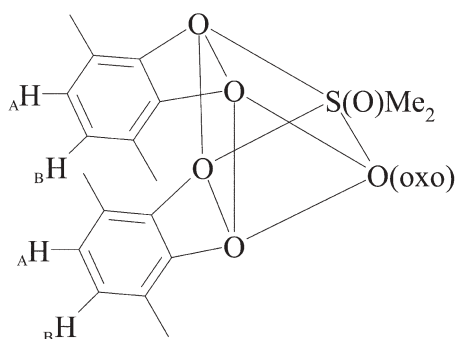


Fig. 18 Bailar twist transition-state in the racemisation of $[\text{Mo}(\text{O})(\text{dmsO})(3,6\text{-DBCat})_2]$. The *tert*-butyl groups omitted for clarity.

proceed *via* a Rây-Dutt transition-state. Only one twist proceeds *via* a Bailar transition-state. Thus magnetisation transfers will be observed between all ligands if the Rây–Dutt twist is operative. If the Bailar twist is operative magnetisation transfer only occurs between one pair of ligands. The twist mechanisms are not mutually exclusive and often occur simultaneously. Accurate measurement of the exchange rates allows the relative contributions of the two twists to be evaluated.⁷⁹

While band shape analysis is often insufficiently sensitive to be able to distinguish between the two twist mechanisms (*e.g.* see reference 80) that is not always the case. In the intermediate exchange regime of the racemisation of $[\text{Mo}(\text{O})(\text{dmsO})(3,6\text{-DBCat})_2]$ (3,6-DBCat = 3,6-di-*tert*-butylcatecholate) and an AB quartet is observed in the ^1H NMR for the catecholate ring hydrogens.⁸¹ The observation of an AB quartet is only consistent with the Bailar twist mechanism (Fig. 18).

On activation with methylaluminumoxane (MAO), the titanium(IV) $[\text{TiCl}_2(\text{O},\text{S},\text{S},\text{O})]$ and $[\text{Ti}(\text{O}^i\text{Pr})_2(\text{O},\text{S},\text{S},\text{O})]$ $\{\text{O},\text{S},\text{S},\text{O} = 1,4\text{-dithiabutanediyl-di}(4,6\text{-disubstituted phenolato})\}$ complexes catalyse styrene polymerisation. The pre-catalyst complexes undergo Λ , Δ racemisation at rates strongly dependent on the nature of the phenolate *ortho*-substituents: the larger the substituent, the slower the rate.⁸² The mechanism of racemisation has not been determined unambiguously, but the authors favour a non-dissociative twist mechanism over a (Ti–S) bond rupture mechanism. The fluxionality, which presumably also occurs in the activated complexes, affects both the efficiency of polymerisation and the polymer tacticity. The more rigid complexes are highly efficient, giving isotactic polystyrene, while the more dynamic (*i.e.* those with smaller *ortho*-substituents) give atactic polystyrene with low activity.

Atropisomerism

Atropisomeric biphenyl-based ligands, such as those depicted in Fig. 19, have found wide-spread use as chiral auxiliaries. Understanding the mechanisms of atropisomerisation and the factors that affect the activation parameters in such complexes is therefore of interest. A number of quite detailed studies have been reported, from which it appears that the precise mechanism differs according to the ligand and/or metal moiety in question.^{83–85}

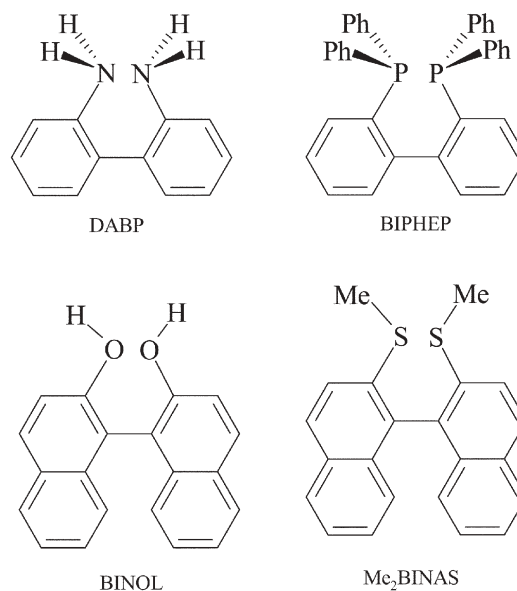
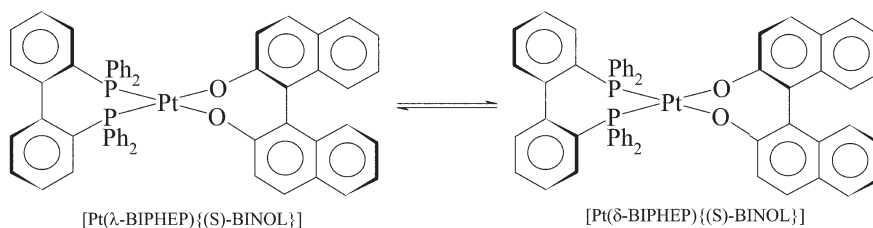


Fig. 19 Examples of atropisomeric biaryl ligands.

Ashby *et al.*⁸³ carried out a detailed 2D EXSY study on the inversion of DABP in $[\text{M}(\eta^6\text{-benzene})\text{Cl}(\text{DABP})]$ ($\text{M} = \text{Ru}$ or Os). Provided the N–H signals can be assigned unambiguously, the different possible exchange *pathways*, namely ligand atropisomerisation, inversion at metal or simultaneous atropisomerisation and metal inversion, can be distinguished from the observed magnetisation transfers. It was thus possible to show that only a ligand atropisomerisation mechanism was operative. Atropisomerisation could occur *via* either a purely conformational change in the seven-membered metalocycle or *via* cleavage of one of the M–N bonds. The latter possibility can, again, be excluded on the basis of the observed magnetisation transfers. In the ‘open’ configuration inversion at the free N atom would be expected to be rapid, which would result in the exchange of the geminal N–H groups: this is not observed (*cf.* N–R group exchange in complexes of hemilabile amine ligands). BINAS atropisomerisation in the $[\text{M}(\text{Me}_2\text{BINAS})\text{X}_2]$ complexes ($\text{M} = \text{Pd}$ or Pt , $\text{X} = \text{Cl}$; $\text{M} = \text{Rh}$, $\text{X}_2 = \text{COD}$) is similarly thought to involve purely conformational changes in the seven-membered chelate ring.⁸⁶

Heating a diastereotopically pure sample of $[\text{Pt}(\lambda\text{-BIPHEP})\{(S)\text{-BINOL}\}]$ in chlorobenzene converted it cleanly to *ca.* 94 : 6 (δ : λ) diastereotopic mixture (Scheme 15).⁸⁵ The free energy of activation for BIPHEP inversion is $\approx 122 \text{ kJ mol}^{-1}$ *cf.* 92 kJ mol^{-1} for the free ligand. The barrier is lowered by *ca.* 20 kJ mol^{-1} in pyridine solvent. In this latter case, an ‘arm-off’ mechanism is proposed, with dissociation of one of the BIPHEP P donor atoms facilitated by the co-ordination of pyridine to the metal centre. An arm-off mechanism may also account for the low barrier (*ca.* $80\text{--}90 \text{ kJ mol}^{-1}$) to BIPHEP atropisomerisation in the 18-electron octahedral ruthenium complex $[\text{RuCl}_2(\text{BIPHEP})(\text{diimine})]$ $\{\text{diimine} = (1S,2S)\text{-1,2-diphenylethane-1,2-diiimine}\}$.⁸⁷ Given the ‘arm-off’ mechanism proposed for BIPHEP atropisomerisation in these complexes, it is noteworthy that, although facile on/off N co-ordination is



Scheme 15 BIPHEP atropisomerisation in [Pt(BIPHEP){(S)-BINOL}].

observed in [Pd(η^3 -allyl)L]⁺ [L = 2-(dicyclohexylphosphino)-2'-(dimethylamino)biphenyl], it is not accompanied by atropisomerisation of the biphenyl ligand.⁸⁸

The observation of a single signal in the ambient temperature ³¹P NMR spectrum of [Co(CO)₃(2,2'-dimethoxyBIPHEP)], in which BIPHEP bridges axial/equatorial positions, is a consequence of a five-coordinate rearrangement,^{89a} similar to that observed in [Rh(CO)₂(H)(P,P)] (P,P = C₂-symmetric diphosphate),^{89b} rather than highly facile BIPHEP inversion.

The possibility of employing (atropisomeric) chiral monodentate ligands as chiral auxiliaries has attracted recent attention. The energy barriers to atropisomerisation in these ligands,^{90–94} together with those for selected biaryl complexes (above) and some organic biphenyls, are collected in Table 5.

Although the possibility of chiral conformations exists in metal-Cp' (Cp' = substituted cyclopentadienyl) complexes, ring rotation is generally too rapid to support chirality. Rates of rotation can be reduced dramatically by employing bulky substituents. More recently, it has been shown that rates can also be reduced significantly in substituted heterometallobenzocenes.^{95,96} At 253 K, the ³¹P NMR spectrum of bis(3,4-dimethyl-2-phenylphosphoryl)titanium dichloride displays two singlets of widely differing intensity owing to the presence of *rac* and *meso* isomers.⁹⁵ The free energy of activation for

rac, *meso* isomerisation, $\Delta G^\ddagger_{298\text{ K}} = 48.1\text{ kJ mol}^{-1}$. Ogasawara and Hayashi⁹⁶ showed that tetra(–)-menthyl]phosphaferrrocene and -ruthenocene existed as a pair of unequally populated, exchanging diastereoisomers at room temperature. The free energies of activation (298 K) are 54.0 and 49.4 kJ mol⁻¹, respectively for the ferrocene and ruthenocene derivatives. The barrier to ring rotation arises from interannular interactions between the bulky Cp substituents. The lower barrier in the ruthenocene complex results from a greater separation of the two phosphoryl rings, due to the larger radius of Ru.

Similarly, the porphyrin ligands in some bis(substituted-porphyrinate) complexes, such as bis(5,15-diarylporphyrinate) cerium(IV)⁹⁷ can interlock causing restricted rotation of the rings, and thereby producing a chiral centre. Relative rotation of the two porphyrin rings leads to racemisation. As in the metallocene complexes, the restriction to rotation is due to steric interactions between the substituents on different rings, and decreasing the size of the metal atom increases the barrier. Thus, for example, while the bis(porphyrin)cerium complexes undergo quite facile racemisation, the corresponding zirconium complexes do not.⁹⁸ It is noteworthy that the addition of acid to the zirconium complex reduces the barrier to rotation significantly, raising the interesting possibility of producing a pH dependent switch.

Table 5 Gibbs free energies of activation for selected atropisomerisations

Compound ^a	$\Delta G^\ddagger/\text{kJ mol}^{-1}$	Reference
[Ru(benzene)Cl(DABP)]	66.8 (283 K)	83
[RuCl ₂ (BIPHEP)(diimine)]	ca. 80–90	87
[Os(benzene)Cl(DABP)]	65.3 (283 K)	83
[Pd(Me ₂ BINAS)Cl ₂]	55 (233 K)	86
[Pt(λ -BIPHEP){(S)-BINOL}] ^b	122 (366 K; C ₆ H ₅ Cl)	85
	ca. 100 (313 K, C ₅ H ₅ N)	85
[Si(BINAP)HMe]	77 (348 K)	90
[Si(BINAP)HEt]	77 (353 K)	90
[Si(BINAP)HPh]	76 (353 K)	90
[Ge(BINAP)HMe]	80 (358 K)	90
[P(BINAP)Ph]	56 (254 K)	94
[P(BINAP)Me]	56 (243 K)	94
[As(BINAP)Ph]	59 (259 K)	94
[As(BINAP)Me]	65 (287 K)	94
[Sb(BINAP)(<i>p</i> -tolyl)]	85 (393 K)	91
[S(BINAP)Me]BF ₄	48	90
5,7-Dihydrodibenzo[<i>c,e</i>]oxepine	38	83, 85
5,7-Dihydrodibenzo[<i>c,e</i>]thiepine	71	83, 85
6,7-Dihydro-5 <i>H</i> -dibenzo[<i>a,c</i>]-cycloheptene	50	83, 85
5,7-Dihydrodibenzo[<i>a,c</i>]cycloheptene-6,6-dicarboxylic acid	98	83, 85

^a See text and Fig. 19 for ligand abbreviations. ^b BIPHEP atropisomerism.

Bimetallic complexes

Alessio and Marzilli have reported the results of detailed structural and dynamic NMR studies on the μ -oxorhenium(V) complexes [Re₂O₃Cl₂(3,5-lut)₄],^{99,100} [Re₂O₃Cl₂(Me₃Bzm)₄],^{99,100} [Re₂O₃Cl₂(py)₂(Me₃Bzm)₂]¹⁰¹ and [Re₂O₃Cl₂(3,5-lut)₂(Me₃Bzm)₂]¹⁰¹ (3,5-lut = 3,5-lutidine; Me₃Bzm = 1,5,6-trimethylbenzimidazole; py = pyridine). In the solid-state structures, which are all analogous, two of the N ligands (one on each Re) are stacked, while the other two can be considered as 'terminal': the solid state structure of *meso*-[Re₂O₃Cl₂(3,5-lut)₂(Me₃Bzm)₂] is shown in Fig. 20.

NMR data indicate that the low temperature (<193 K) solution structures are very similar to those observed in the solid-state but on warming complex dynamic behaviour, involving rotations about the Re–O–Re and Re–N bonds becomes apparent. In the [Re₂O₃Cl₂L₄] and *meso*-[Re₂O₃Cl₂L₂L'₂] complexes *synchronous* ca. 180° and 90° rotations about the Re–O–Re and Re–N bonds, respectively, leads to racemisation of the dimers, while in *rac*-[Re₂O₃Cl₂L₂L'₂] it leads to the interconversion of two chiral rotamers.

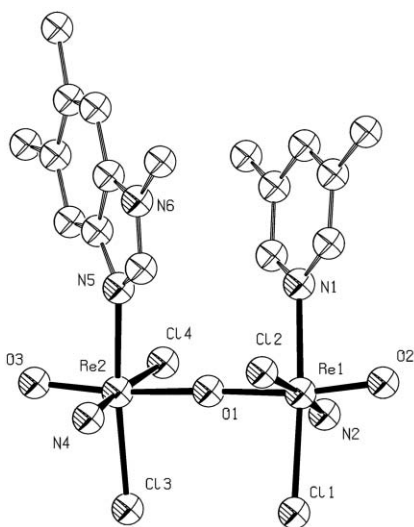


Fig. 20 ORTEP plot (arbitrary ellipsoid probability) of *meso*-[Re₂O₃Cl₂(3,5-lut)₂(Me₃Bzm)₂] showing the stacked ligands. The carbon atoms of the 'terminal' ligands and C atom labels omitted for clarity.

References

- 1 R. S. Berry, *J. Chem. Phys.*, 1960, **32**, 933.
- 2 E. W. Abel, S. K. Bhargava and K. G. Orrell, *Prog. Inorg. Chem.*, 1984, **32**.
- 3 K. G. Orrell, *Coord. Chem. Rev.*, 1989, **96**, 1.
- 4 K. G. Orrell, V. Šik and D. Stephenson, *Prog. Nucl. Magn. Reson. Spectrosc.*, 1990, **22**, 141.
- 5 E. W. Abel and K. G. Orrell, *Encyclopedia of Inorganic Chemistry*, ed. R. B. King, Wiley, New York, 1994, Vol. 5, p. 2581.
- 6 F. J. Faller, *Encyclopedia of Inorganic Chemistry*, ed. R. B. King, Wiley, New York, 1994, Vol. 8, p. 3914.
- 7 K. G. Orrell, *Ann. Rep. NMR Spectrosc.*, 1999, **37**, 1.
- 8 J. W. Faller, *Encyclopedia of Inorganic Chemistry*, ed. R. B. King, Wiley, New York, 2nd Edn, 2005, Vol. 8, p. 5270.
- 9 A. D. Bain, *Prog. Nucl. Magn. Reson. Spectrosc.*, 2003, **43**, 63 and references therein.
- 10 A. D. Horton and J. H. G. Frijns, *Angew. Chem., Int. Ed. Engl.*, 1991, **30**, 1152.
- 11 A. Bonny, R. D. Hunter and S. R. Stobart, *J. Am. Chem. Soc.*, 1982, **104**, 1855.
- 12 D. L. Davies, J. Fawcett, S. A. Garratt and D. R. Russell, *J. Organomet. Chem.*, 2002, **662**, 43.
- 13 H. Asano, K. Katayama and H. Kurosawa, *Inorg. Chem.*, 1996, **35**, 5760.
- 14 D. L. Davies, J. Fawcett, S. A. Garratt and D. R. Russell, *Organometallics*, 2001, **20**, 3029.
- 15 V. Alezra, G. Bernardinelli, C. Corminboeuf, U. Frey, E. P. Kündig, A. E. Merbach, C. M. Saudan, F. Viton and J. Weber, *J. Am. Chem. Soc.*, 2004, **126**, 4843.
- 16 T. R. Ward, O. Schafer, C. Daul and P. Hofmann, *Organometallics*, 1997, **16**, 3207.
- 17 E. P. Kündig, C. M. Saudan, V. Alezra, F. Viton and G. Bernardinelli, *Angew. Chem., Int. Ed.*, 2001, **40**, 4481.
- 18 E. P. Kündig, C. M. Saudan and G. Bernardinelli, *Angew. Chem., Int. Ed.*, 1999, **38**, 1220.
- 19 D. L. Davies, J. Fawcett, S. A. Garratt and D. R. Russell, *Dalton Trans.*, 2004, 3629.
- 20 H. Brunner, K. Kollnberger, T. Burgemeister and M. Zabel, *Polyhedron*, 2000, **19**, 1519.
- 21 H. Brunner, R. Oeschey and B. Nuber, *J. Chem. Soc., Dalton Trans.*, 1996, 1499.
- 22 H. Brunner, R. Oeschey and B. Nuber, *J. Organomet. Chem.*, 1996, **518**, 47.

- 23 H. Brunner, T. Neuhierl and B. Nuber, *J. Organomet. Chem.*, 1998, **563**, 173.
- 24 H. Brunner, P. Faustmann and B. Nuber, *J. Organomet. Chem.*, 1998, **556**, 129.
- 25 H. Brunner, P. Faustmann, A. Dietl and B. Nuber, *J. Organomet. Chem.*, 1997, **542**, 255.
- 26 P. Braunstein and F. Naud, *Angew. Chem., Int. Ed.*, 2001, **40**, 680.
- 27 E. W. Abel, V. S. Dimitrov, N. J. Long, K. G. Orrell, A. G. Osborne, H. M. Pain and V. Šik, *J. Chem. Soc., Dalton Trans.*, 1993, 291.
- 28 E. R. Civitello, P. J. Dragovich, T. B. Karpishin, S. G. Novick, G. Bierach, J. F. O'Connell and T. D. Westmoreland, *Inorg. Chem.*, 1993, **32**, 237.
- 29 E. W. Abel, K. G. Orrell, A. G. Osborne, V. Šik, M. B. Hursthouse and K. M. A. Malik, *J. Chem. Soc., Dalton Trans.*, 1994, 3441.
- 30 E. Rotondo, G. Giordano and D. Minniti, *J. Chem. Soc., Dalton Trans.*, 1996, 253.
- 31 R. Romeo, A. Grassi and L. M. Scolaro, *Inorg. Chem.*, 1992, **31**, 4383.
- 32 P. J. Heard and C. Jones, *J. Chem. Soc., Dalton Trans.*, 1997, 1083.
- 33 P. J. Heard and D. A. Tocher, *J. Chem. Soc., Dalton Trans.*, 1998, 2169.
- 34 P. Braunstein, F. Naud, A. Dedieu, M.-M. Rohmer, A. DeCian and S. J. Rettig, *Organometallics*, 2001, **20**, 2966.
- 35 P. J. Heard, P. M. King, A. D. Bain, P. Hazendonk and D. A. Tocher, *J. Chem. Soc., Dalton Trans.*, 1999, 4495.
- 36 P. J. Heard, P. M. King and D. A. Tocher, *J. Chem. Soc., Dalton Trans.*, 2000, 1769.
- 37 P. J. Heard, P. M. King, P. Sroisuwat and N. Kaltsoyannis, *Polyhedron*, 2003, **22**, 3371.
- 38 P. J. Heard, P. M. King, A. D. Bain and P. Hazendonk, *Can. J. Chem.*, 1999, **77**, 1707.
- 39 J. L. Bookham, D. M. Smithies and M. T. Pett, *J. Chem. Soc., Dalton Trans.*, 2000, 975.
- 40 H. Yang, N. Lugan and R. Mathieu, *Organometallics*, 1997, **16**, 2089.
- 41 (a) H.-J. Gais, P. R. Burns, G. Raabe, R. Hainz, M. Schleusner, J. Runsink and G. S. Babu, *J. Am. Chem. Soc.*, 2005, **127**, 6617; (b) H.-J. Gais, R. Hainz, H. Müller, P. R. Burns, N. Giesen, G. Raabe, J. Runsink, S. Nienstedt, J. Decker, M. Schleusner, J. Hachtel, C.-W. Woo and P. Das, *Eur. J. Org. Chem.*, 2000, 3973.
- 42 G. Tresoldi, L. Baradello, S. Lanza and P. Cardiano, *Eur. J. Inorg. Chem.*, 2005, 2423.
- 43 S. Toyota, T. Nakamata, N. Nitta and F. Ito, *Chem. Lett.*, 2004, **33**, 206.
- 44 S. Toyota, F. Ito, N. Nitta and T. Nakamata, *Bull. Chem. Soc. Jpn.*, 2004, **77**, 2081.
- 45 L. Balazs, O. Stanga, H. J. Breunig and C. Silvestru, *Dalton Trans.*, 2003, 2237.
- 46 N. Gül and J. H. Nelson, *J. Mol. Struct.*, 1999, **475**, 121.
- 47 S. Attar, J. H. Nelson and J. Fischer, *Organometallics*, 1995, **14**, 4476.
- 48 I. C. M. Wehman-Ooyevaar, J. A. Vedral, J. T. B. H. Jastrzebski, D. M. Grove and G. van Koten, *J. Organomet. Chem.*, 1993, **451**, 195.
- 49 J. T. B. H. Jastrzebski, J. Boersma and G. van Koten, *J. Organomet. Chem.*, 1991, **413**, 43.
- 50 H. Höpfl, N. Farfán, D. Castillo, R. Santillan, R. Contreras, F. J. Metínez-Metínez, M. Galván, R. Alvarez, L. Fernández, H. Halut and J.-C. Daran, *J. Organomet. Chem.*, 1997, **544**, 175.
- 51 H. Höpfl, N. Farfán, D. Castillo, R. Santillan, A. Gutierrez and J.-C. Daran, *J. Organomet. Chem.*, 1998, **553**, 221.
- 52 P. Shao, R. A. L. Gendon and D. J. Berg, *Can. J. Chem.*, 2000, **78**, 255.
- 53 X. Bei, D. C. Swenson and R. F. Jordan, *Organometallics*, 1997, **16**, 3282.
- 54 P. Shao, R. A. L. Gendon, D. J. Berg and G. W. Bushnell, *Organometallics*, 2000, **19**, 509.
- 55 T. Yamamoto and T. Iijima, *J. Organomet. Chem.*, 2004, **689**, 2421.
- 56 A. Chandrasekaran, R. O. Day and R. R. Holmes, *J. Am. Chem. Soc.*, 2000, **122**, 1066.

- 57 A. Chandrasekaran, R. O. Day and R. R. Holmes, *Inorg. Chem.*, 2000, **39**, 5683.
- 58 N. V. Timosheva, A. Chandrasekaran, R. O. Day and R. R. Holmes, *Organometallics*, 2000, **19**, 5614.
- 59 N. V. Timosheva, A. Chandrasekaran, R. O. Day and R. R. Holmes, *Phosphorus, Sulfur Silicon Relat. Elem.*, 2001, **168**, 59.
- 60 K. C. Fortner, J. P. Bigi and S. N. Brown, *Inorg. Chem.*, 2005, **44**, 2803.
- 61 B. R. Manzano, F. A. Jalón, F. Gómez-de la Torre, A. M. López-Agenjo, A. M. Rodríguez, K. Mereiter, W. Weissensteiner and T. Sturm, *Organometallics*, 2002, **21**, 789.
- 62 F. A. Jalón, B. R. Manzano, F. Gómez-de la Torre, A. M. López-Agenjo, A. M. Rodríguez, K. Mereiter, T. Sturm, J. Mahia and M. Maestro, *J. Chem. Soc., Dalton Trans.*, 2001, 2417.
- 63 F. Gómez-de la Torre, F. A. Jalón, A. M. López-Agenjo, B. R. Manzano, A. Rodríguez, T. Sturm, W. Weissensteiner and M. Martínez-Ripoll, *Organometallics*, 1998, **17**, 4634.
- 64 R. Fernández-Galán, F. A. Jalón, B. R. Manzano, J. Rodríguez-de la Fuente, M. Vrahami, B. Jedlicka, W. Weissensteiner and G. Jögl, *Organometallics*, 1997, **16**, 3758.
- 65 M. Valentini, K. Selvakumar, M. Wörle and P. S. Pregosin, *J. Organomet. Chem.*, 1999, **587**, 244 and references therein.
- 66 (a) J. Elgero, A. Fruchier, A. de la Hoz, F. A. Jalón, B. R. Manzano, A. Otero and F. Gómez-de la Torre, *Chem. Ber.*, 1996, **129**(589), 2; (b) F. Gómez-de la Torre, A. de la Hoz, F. A. Jalón, B. R. Manzano, A. Otero, A. M. Rodríguez, M. C. Rodríguez-Pérez, A. Echevarria and J. Elguero, *Inorg. Chem.*, 1998, **37**, 6606; (c) F. Gómez-de la Torre, A. de la Hoz, F. A. Jalón, B. R. Manzano, A. M. Rodríguez, J. Elguero and M. Martínez-Ripoll, *Inorg. Chem.*, 2000, **39**, 115; (d) J. Guerrero, F. Gómez-de la Torre, A. de la Hoz, F. A. Jalón, B. R. Manzano and A. Rodríguez, *New J. Chem.*, 2001, **25**, 1050.
- 67 R. Romeo, L. Fenech, L. Monsù, M. Scolaro, A. Albinati, A. Macchioni and C. Zuccaccia, *Inorg. Chem.*, 2001, **40**, 3239.
- 68 H. Yang, M. Alvarez-Gresier, N. Lugan and R. Mathieu, *Organometallics*, 1997, **16**, 1401.
- 69 M. Tamm, T. Bannenberg, B. Dressel, R. Fröhlich and C. Holst, *Inorg. Chem.*, 2002, **41**, 47.
- 70 A. S. Batsanov, J. I. Bruce, T. Ganesh, P. J. Low, R. Katakay, H. Puschmann and P. G. Steel, *J. Chem. Soc., Perkin Trans. 1*, 2002, 932.
- 71 P. N. O'Shaughnessy, K. M. Gillespie, P. D. Knight, I. J. Munslow and P. Scott, *Dalton Trans.*, 2004, 2251.
- 72 A. A. H. van der Zeijden, C. Mattheis and R. Fröhlich, *Organometallics*, 1997, **16**, 2651.
- 73 A. Steudel, E. Siebel, R. D. Fischer, G. Paolucci and V. Lucchini, *J. Organomet. Chem.*, 1988, **556**, 229.
- 74 A. Steudel, J. Stehr, E. Siebel and R. D. Fischer, *J. Organomet. Chem.*, 1998, **570**, 89.
- 75 N. Feiken, P. Pregosin and G. Trabesinger, *Organometallics*, 1998, **17**, 4510.
- 76 P. I. Arvidsson, P. Ahlberg and G. Hilmersson, *Chem.-Eur. J.*, 1999, **5**, 1348 and references therein.
- 77 P. I. Vrvdsson, G. Hilmersson and P. Ahlberg, *J. Am. Chem. Soc.*, 1999, **121**, 1883.
- 78 K. Kite, K. G. Orrell, V. Šik and Y. Roger, *Polyhedron*, 1995, **14**, 2711 and references therein.
- 79 M. Gromova, O. Jarjayes, S. Hamman, R. Nordin, C. Béguin and R. Willem, *Eur. J. Inorg. Chem.*, 2000, 544.
- 80 D. J. Berg, C. Zhou, T. Barlay, X. Fei, S. Feng, K. A. Ogilvie, R. A. Gossage, B. Twamley and M. Wood, *Can. J. Chem.*, 2005, **83**, 449.
- 81 C.-M. Liu, E. Nordlander, D. Schmech, R. Shoemaker and C. G. Pierpont, *Inorg. Chem.*, 2004, **43**, 2114.
- 82 C. Capacchione, R. Manivannan, M. Barone, K. Beckerle, R. Centore, L. Oliva, A. Proto, A. Tuzi, T. P. Spaniol and J. Okuda, *Organometallics*, 2005, **24**, 2971.
- 83 S. S. Alguindigue, M. A. Khan and M. T. Ashby, *Organometallics*, 1999, **18**, 5112.
- 84 M. Ringwald, R. Stürmer and H. H. Brintzinger, *J. Am. Chem. Soc.*, 1999, **121**, 1524.
- 85 M. D. Tudor, J. J. Becker, P. S. White and M. R. Gagné, *Organometallics*, 2000, **19**, 4376.
- 86 S. Gladiali, D. Fabbri, L. Kollar, C. Claver, N. Ruiz, A. Alvarez-Loarena and J. F. Piniella, *Eur. J. Inorg. Chem.*, 1998, 113.
- 87 K. Mikami, T. Korenaga, M. Terada, T. Ohkuma, T. Pham and R. Noyori, *Angew. Chem., Int. Ed.*, 1999, **39**, 495.
- 88 J. W. Faller and N. Sarantopoulos, *Organometallics*, 2004, **23**, 2008.
- 89 (a) T. M. Schmid, S. Gischig and G. Consiglio, *Chirality*, 2005, **17**, 353; (b) G. J. H. Buisman, L. A. van der Veen, P. C. J. Kamer and P. W. N. M. van Leeuwen, *Organometallics*, 1997, **16**, 5681.
- 90 S. Yasuike, T. Iida, S. Okajima, K. Yamaguchi, H. Seki and J. Kurita, *Tetrahedron*, 2001, **57**, 10047.
- 91 S. Yasuike, T. Iida, S. Okajima, K. Yamaguchi, H. Seki and J. Kurita, *Tetrahedron Lett.*, 2001, **42**, 441.
- 92 S. Gladiali, D. Fabbri, G. Banditelli, M. Manassero and M. Sansoni, *J. Organomet. Chem.*, 1994, **475**, 307.
- 93 K. Tani, H. Tashiro, M. Yoshida and T. Yamagata, *J. Organomet. Chem.*, 1994, **469**, 229.
- 94 A. A. Watson, A. C. Willis and S. B. Wild, *J. Organomet. Chem.*, 1993, **445**, 71.
- 95 T. K. Hollis, Y. Joon Ahn and F. S. Tham, *Chem. Commun.*, 2002, 2996.
- 96 M. Ogasawara, K. Yoshida and T. Hayashi, *Organometallics*, 2003, **22**, 1783.
- 97 K. Tashiro, T. Fujiwara, K. Konishi and T. Aida, *Chem. Commun.*, 1998, 1121.
- 98 K. Tashiro, K. Konishi and T. Aida, *Angew. Chem., Int. Ed. Engl.*, 1997, **36**, 856.
- 99 L. G. Marzilli, M. Iwamoto, E. Alessio, L. Hansen and M. Calligaris, *J. Am. Chem. Soc.*, 1994, **116**, 815.
- 100 E. Alessio, L. Hansen, M. Iwamoto and L. G. Marzilli, *J. Am. Chem. Soc.*, 1996, **118**, 7593.
- 101 E. Alessio, E. Zangrando, E. Iengo, M. Macchi, P. A. Marzilli and L. G. Marzilli, *Inorg. Chem.*, 2000, **39**, 294.